

Response to reviewer #1

Thank you for the careful and thorough reading of this manuscript and your thoughtful comments and suggestions. Our responses follow the reviewer's comments (in *Italics*).

General comments:

There are a number of recent papers on the topic of NO_x emission trends in the United States as observed from space and as compared to predictions from models. The papers raise issues about the emission models, about the resolution of measurements and models needed to derive accurate trends, about interpretation of satellite observations including whether and how the regional background is included in the trend analysis, and whether the lifetime of NO_x is also changing with time affecting interpretation of temporal trends. The analysis in this paper focuses on nonlinearities in chemistry which is related to the question of chemical lifetime. The analysis in the paper seems solid and the discussion and conclusions try to put the paper in context of the recent literature.

I recommend the abstract be revisited in light of the discussion and conclusions as nowwritten.

Reply:

Thank you for your suggestion. We listed the factors affecting the nonlinear relationships among anthropogenic NO_x emissions, NO₂ surface concentrations, and NO₂ TVCDs in Lines 17 - 18 in the revised manuscript. Not only chemistry and background sources but also physical processes, such as transport, contribute to the nonlinearities.

I also recommend the authors consider whether they can make some more general conclusions about the role of nonlinearities that are the focus of their work as a guide to future research. For example does this research help push forward the conversation about the model resolution needed to describe NO_x to a specified accuracy? Other papers suggest that 36km might not be sufficient for the absolute accuracy the authors are trying to achieve. On the other hand there might be cancellation of errors in computation of trends that allows use of lower resolution for questions about trends?

Reply:

We think 36 km is sufficient for the regional analysis in this study. A higher resolution model result will not change the nonlinearity discussion in section 3.1. The low-anthropogenic-NO_x emission regions are more sensitive to various factors, such as lightning and soil NO_x emissions and transport, than high-anthropogenic-NO_x emission regions. The critical thing in trend analysis using satellite data directly is therefore to use the data over high-anthropogenic-NO_x emission regions and avoid low-anthropogenic-NO_x emission regions. Therefore, the favorable resolution depends on the emission distributions of the study area. The model analysis used here is only to show the problems associated with using data over the low-anthropogenic-NO_x emission regions. Silvern et al. (2019) used modeling results with a resolution of $0.5^{\circ} \times 0.625^{\circ}$ and shown that the tropospheric NO_x lifetime decreased from 8.1 hours to 7.7 hours from 2005 – 2017. When using high-resolution simulations, suggested by Valin et al. (2011), the required accuracy on the anthropogenic emission distribution is much higher than 36 km. Our model results using 4- and 36-km resolutions indicate that the errors of 4-km

NO_x emission distribution are significant and need to be accounted for in modeling analysis. It is beyond what is of interest in this study.

References

Silvern, R. F., Jacob, D. J., Mickley, L. J., Sulprizio, M. P., Travis, K. R., Marais, E. A., Cohen, R. C., Laughner, J. L., Choi, S., Joiner, J., and Lamsal, L. N.: Using satellite observations of tropospheric NO₂ columns to infer long-term trends in US NO_x emissions: the importance of accounting for the free tropospheric NO₂ background, *Atmos. Chem. Phys.*, 19, 8863-8878, 10.5194/acp-19-8863-2019, 2019.

Valin, L. C., Russell, A. R., Hudman, R. C., and Cohen, R. C.: Effects of model resolution on the interpretation of satellite NO₂ observations, *Atmos. Chem. Phys.*, 11, 11647-11655, 10.5194/acp-11-11647-2011, 2011.

Response to reviewer #2

We thank the reviewer for careful and thorough reading of this manuscript and the thoughtful comments and suggestions. Our answers follow the reviewer's comments (in *Italics*).

General comments:

There has been many studies in the last years on the recent trends of NO_x emissions over the U.S., the main motivation being the apparent important change in NO₂ column trend since 2010, which obviously requires careful analysis using the available data as well as using models. The present study is useful, as it clearly shows that there is no significant discrepancy between the NEI emission trends and the different NO₂ (surface and column) data, when considering only urban areas. The paper discusses the non-linear relationship between NO_x emissions and NO₂ abundances. Model calculations using REAM at 36kmx36 km are used to illustrate this point and show that the feedbacks are much stronger at low-NO_x than at high-NO_x. Although the relevance of NO_x natural emissions (which obviously do not have the same trends as the anthropogenic component) is mentioned, the paper does not dwell on it.

In fact, and this is my main comment, I think clarifications are needed in order to sort out the respective roles of chemical non-linearities and the existence of the background. Both natural emissions and chemical non-linearities play their largest role during summer over rural areas, and more so in the free troposphere than near the surface. But it is not entirely clear from the paper how much these two main factors contributed to

the apparent discrepancy between the different sets of trends. This should be clarified.

Reply:

Thank you for your suggestions. Since in our trend analyses in Section 3.3, we chose urban regions with small β and γ values and had minimized the impacts of chemical nonlinearity and background sources on inferring anthropogenic NO_x emissions from satellite datasets. Silvern et al. (2019) also show that lightning NO_x and the lifetime of tropospheric NO_x have no significant trend signals from 2005 – 2017. We think you ask which factors affect β and γ more.

Due to the interactions among NO_x emissions, chemistry, and physical processes, it is difficult to completely and accurately separate the effects of all factors to β and γ values. Here, we estimated the impact of background sources and non-emission factors (transport, chemistry, and wet and dry depositions) on β and γ values and added two supplement figures (Figures S6 and S7) in Lines 105 – 143 in the revised supplement figure file. The supplement figure citation was updated in the manuscript. We also added “transport” in Line 241. Figures S6 and S7 show that the contributions of both background sources and non-emission factors to β and γ values are much more significant in low-anthropogenic- NO_x emission regions than high-anthropogenic- NO_x emission regions. In general, non-emission factors contribute more to the nonlinearity than background sources in low-anthropogenic- NO_x emission regions (Figures S7c and S7d) except for the first bin (of low local emissions) where background sources contribute more to the nonlinearity than non-emission factors at 10:00 – 11:00 LT. We added the discussion about the contributions of the two factors to β and γ values in Lines

231 – 237 and Lines 257 – 264.

Also, although the paper mentions the use of observed NO_3^- deposition trends to further support the declining trend of NO_x emissions, it would be useful to incorporate more explicitly this information in the discussion.

Reply:

We mentioned nitrate wet deposition fluxes in the introduction in Lines 43 - 47 in the revised manuscript to support the decrease of NO_x emissions from the mid-2000s to the 2010s based on previous researches. Now we added a new supplement Figure S1 based on the National Acid Deposition Program (NADP) observations over the CONUS in Lines 75 – 79 in the revised supplement figure file, which shows a decrease ($\sim 30\%$ - $\sim 40\%$) of nitrate wet deposition fluxes from 2003 – 2017. In addition, we mentioned in Lines 376 - 378 in the revised manuscript that Silvern et al. (2019) used nitrate wet deposition fluxes in their analyses. Unlike the study of Silvern et al., which have multiyear simulation results and can compare model results with nitrate wet deposition flux observations, we ran 1-month simulation to show the nonlinearities among anthropogenic NO_x emissions, NO_2 surface concentrations, and NO_2 TVCDs to support the separation between urban and rural regions in our trend analyses. As discussed in Silvern et al. (2019), nitrate wet deposition fluxes are affected by both boundary NO_x and free-tropospheric NO_x , and most nitrate wet deposition flux sites are in rural regions. We didn't find any significant improvement from rural to urban regions when comparing nitrate wet deposition fluxes with coincident OMI-QA4ECV NO_2 TVCDs as shown in Figure R1 (Urban: $\text{TVCD} = 1.13 \times \text{NADP} + 0.13$, $R^2 = 0.84$; Rural: $\text{TVCD} =$

$1.49 \times \text{NADP} - 0.11$, $R^2 = 0.82$), which is a key point of our study. We suggest reading Silvern et al. paper for more details about nitrate wet deposition fluxes.

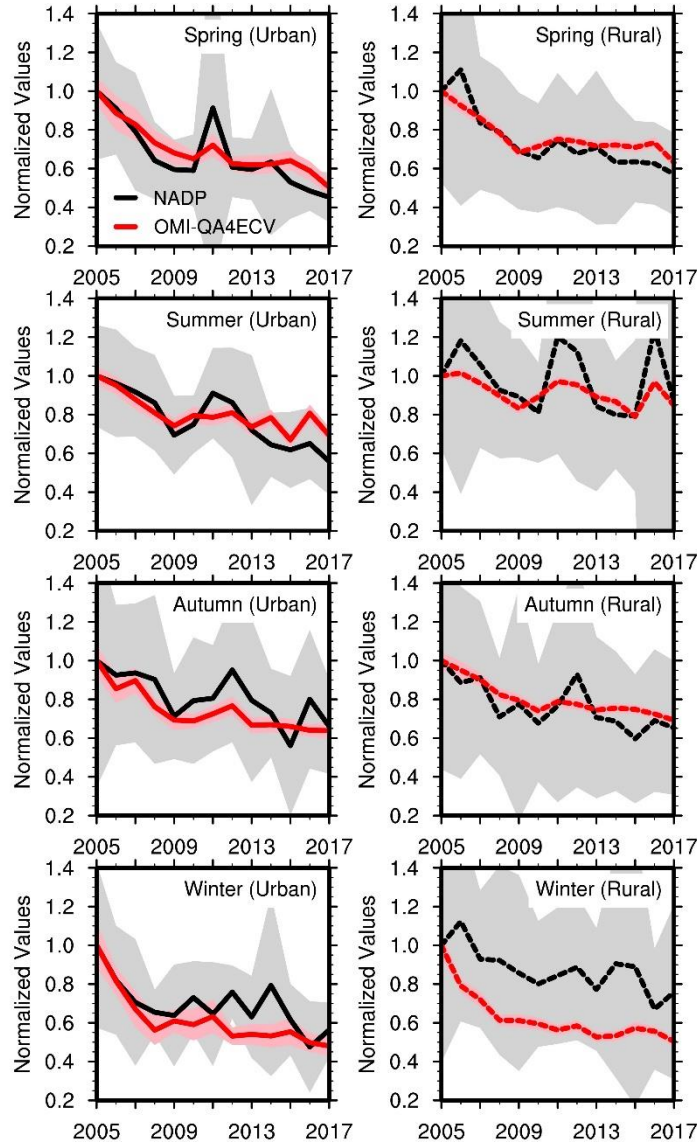


Figure R1. Relative annual variations of NADP nitrate wet deposition fluxes and coincident OMI-QA4ECV NO₂ TVCD in each season from 2005 – 2017 for urban (left panel) and rural (right panel) regions. The observation data are scaled by the corresponding 2005 values. Black and red lines denote NADP nitrate wet deposition fluxes and OMI-QA4ECV NO₂ TVCDs, respectively. Shading in a lighter color is added

to show the standard deviation of the results.

Additional (minor) comments:

- l. 34, the total of 0.24 Tg N for natural NO_x emissions seems to be very low, where does it come from? I don't think NEI2014 provides this information. Please provide separately the soil, biomass burning and lightning emission information.

Reply:

Thank you for your suggestion. Unlike the natural NO_x sources from Seinfeld and Pandis (2016), which includes both lightning and soil NO_x emissions, NEI2014 only provides soil NO_x emissions calculated by the Biogenic Emission Inventory System (BEIS) but no lightning NO_x emissions (EPA, 2018). The 0.24 Tg N of natural NO_x emissions refers to soil NO_x emissions. We changed “anthropogenic and natural NO_x” to “anthropogenic and soil NO_x” in Line 35. And we provided soil and lightning NO_x emissions from REAM over the CONUS in July 2011 in Lines 112 – 115 in the revised manuscript.

- l. 64-65: there are earlier references for the effect of non-linearities on NO₂ trends

Reply:

Yes, we added a citation of Lamsal et al. (2011). Please see Lines 65 – 66 in the revised manuscript.

- section 2.1 on REAM. What is the model domain?

Reply:

The model domain is shown in Figure 3, covering the CONUS. We added “the model domain of which is shown in Figure 3” in Line 95 in the revised manuscript to show the model domain.

- l. 96: How is meteorology constrained by NCEP?

Reply:

NCEP CFSv2 datasets provide initial and boundary conditions for our WRF simulation.

- l. 100-102 it's a detail, but it seems a little strange that weekday emissions are based on NEI while weekend values are reduced. Isn't NEI an average?

Reply:

Our NEI2011 emission inventory is from PNNL and has an initial horizontal resolution of 4 km. We re-gridded it to 36 km. The emission inventory was calculated by using the Sparse Matrix Operator Kernel Emissions (SMOKE) model which could produce hourly emissions for each day, thus could separate weekdays and weekends. We obtained only averaged weekday emissions from PNNL but no weekend emissions. Therefore, we scaled the weekend emissions based on previous studies (Beirle et al., 2003; Boersma et al., 2009; Choi et al., 2012; DenBleyker et al., 2012; Herman et al., 2009; Judd et al., 2018; Kaynak et al., 2009; Kim et al., 2016) and our model evaluations with observations. Currently, GEOS-Chem and CMAQ provide hourly anthropogenic emissions for each day for NEI2011 and NEI2014, respectively, such as NEI2014v2 at

https://www.aocom.ucar.edu/Models/EPA/cmaq_cb6/all/. NEI2005 at ftp://aftp.fsl.noaa.gov/divisions/taq/emissions_data_2005/ also provides weekday, Saturday, and Sunday emissions separately.

- l. 105 what about lightning emissions?

Reply:

We described the method to calculate lightning NO_x emissions in Lines 107 – 112 in the revised manuscript.

- l. 148-149 the requirement that RCI > 50% is quite strict. What happens to the trends when you change that?

Reply:

When we changed the criterion to RCI < 100%, about 17% of seasonal data were removed. The following Figure R2 is for RCI < 100%. In Figure R3, we included all seasonal data with any RCI values. Generally, the trends of satellite NO₂ TVCDs over urban regions are still consistent with the trends of EPA NO_x emissions and surface NO₂ measurements in both Figure R2 and Figure R3, although there are some differences among Figure R2, Figure R3, and Figure 6 in the main manuscript. It emphasizes the selection of urban regions in trend analyses. Here, we would like to keep the RCI < 50% criterion in the main manuscript as it removes the effects of outliers.

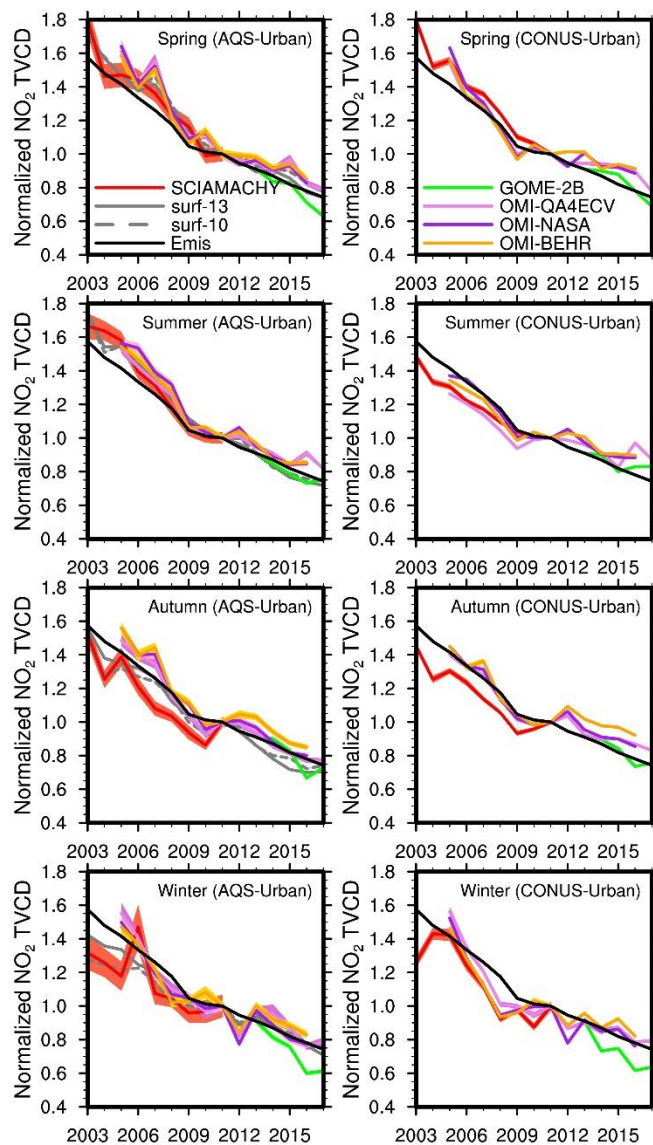


Figure R2. Same as Figure 6 in the main manuscript, but for $\text{RCI} < 100\%$.

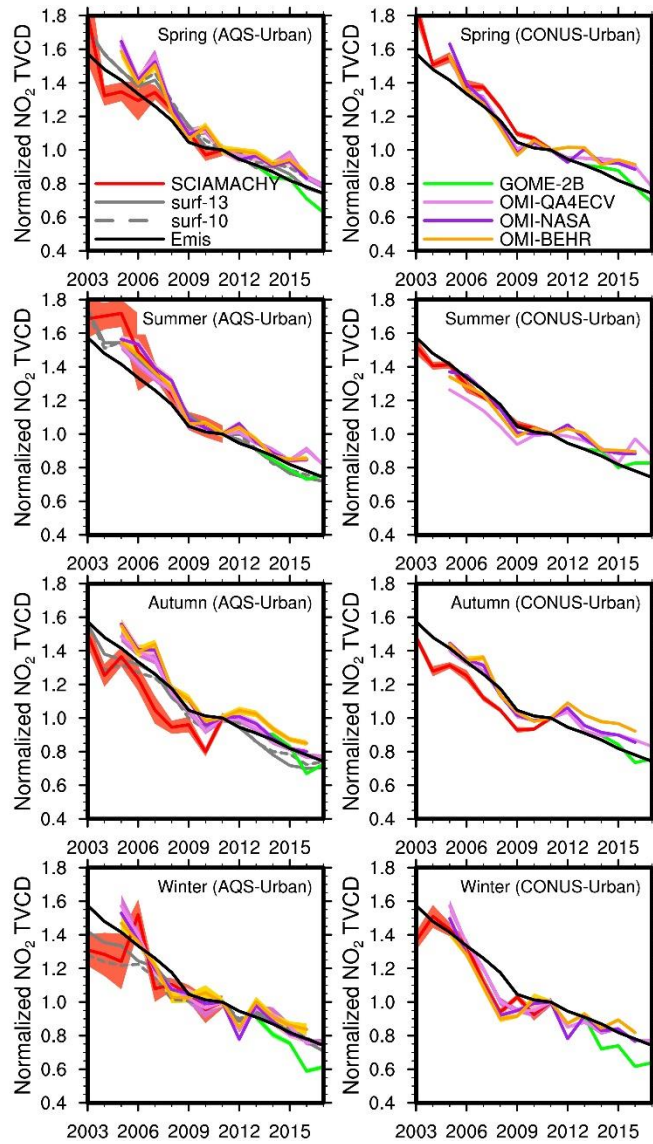


Figure R3. Same as Figure 6 in the main manuscript, but for all seasonal data with any RCI values.

- l. 184 how many measurements are rejected from this conditions on RCI?

Reply:

For surface concentrations, due to the completeness and stability of surface measurements, almost all seasonal averages (98.5%) satisfy the $RCI < 50\%$ criterion.

We added the information in Lines 194 – 195 in the revised manuscript.

- l. 202 Are the β and γ calculated based on total emissions with or without lightning emissions? Lightning contributes significantly to the total column, but very little to surface concentrations (in part due to the vertical dependence of spaceborne instruments sensitivity).

Reply:

Yes. Surface NO_2 concentrations are not much affected by NO_x in the free troposphere, which NO_2 in the free troposphere is an important component of NO_2 TVCD. We have discussed it in Lines 248 – 251. Both β and γ are calculated based on the emissions without lightning. The lifetime of lightning NO_x in the free troposphere is much longer than that in the boundary layer. As mentioned above, we added two supplement figures (Figures S6 and S7) to evaluate the contributions of different factors to β and γ values.

- l. 229 "such as NO_x transport from nearby regions" this is surprising since the calculated sensitivities were said to be purely local

Reply:

In Lines 225 – 226 in the revised manuscript, we said, “Using this procedure, the effects of anthropogenic NO_x emission reduction were localized”. It doesn’t mean that transport effect is eliminated. Let’s think about a simple example, to calculate β and γ values for a single grid cell “A”, we only need to adjust the NO_x emissions of “A” but keep all other grid cells the same as before. By comparing two simulations, one with the original

emissions, the other one with grid cell “A” adjusted, we can obtain the β and γ values of “A”. Here, only the NO_x emissions of “A” are reduced in the adjusted simulation, and other grid cells are unchanged, so the emission reduction effect is localized. But transport still makes effects. Outfluxes from “A” to nearby grid cells will be different from the original simulation, as NO_x concentrations in “A” change. Our method described in Lines 216 – 225 in the revised manuscript can simulate the above procedure simultaneously for all grid cells and save computing time. This idea is different from a method widely used in previous studies by comparing one simulation with original emissions and the other one with emission reductions for all grid cells, where not only outfluxes from “A” change but also influxes to “A” are different from the original simulation. That is to say, the emission reductions of nearby grids are affecting grid cell “A”, which cannot be used to calculate local β and γ values.

l. 234 there is no "transport effect". β and γ are closer to 1 at 10-11 LT (compared to 13-14 LT) because of the weaker chemical losses.

Reply:

As we explained in the above answer, there are transport effects in the calculation of β and γ . In Line 234 in the original manuscript (Lines 251 – 253 in the revised manuscript), we were talking about the uncertainties of β and γ in each bin, and generally we don't have enough evidence from Figure 2 to show that β and γ are closer to 1 at 10-11 LT compared to 13-14 LT.

l. 242 I suppose the "urban" definition depends on anthropogenic NO_x emissions on a

specific year (and month maybe). This should be specified.

Reply:

Thank you for your suggestion. Yes, the definition is based on NEI2011, as described in Section 2.1, which provides annual average emissions for 2011 weekdays. We changed “anthropogenic NO_x emissions “ to “anthropogenic NO_x emissions from NEI2011” to make it clear. Please see Lines 268 – 269 in the revised manuscript.

l. 330-332 Note that only 22 AQS sites (out of 179) are rural. Therefore, is the difference between this study and the results of Lamsal et al. and Jiang et al. really due to the selection of urban sites?

Reply:

Figure R4 shows the comparison between mean NO₂ concentrations from AQS urban sites and those from all (urban + rural) AQS sites, and there is no significant difference. Silvern et al. (2019) suggested that Jiang et al. (2018) included those sites with incomplete measurement records, which might be the reason why Jiang et al. (2018) had lower slowdown magnitude compared to our study (Table 1 in the main manuscript) and Silvern et al. (2019). The decreasing rates of AQS NO₂ concentrations in Lamsal et al. (2015) (Table 1 in the main manuscript) are smaller than our study and Silvern et al. (2019) (2005 – 2009: $-6.6 \pm 1.2\% \text{ a}^{-1}$; 2011 – 2015: $-4.5 \pm 1.7\% \text{ a}^{-1}$), which might also be partly due to their different data processing procedure. We changed the original sentence, please see Lines 356 – 361 in the revised manuscript.

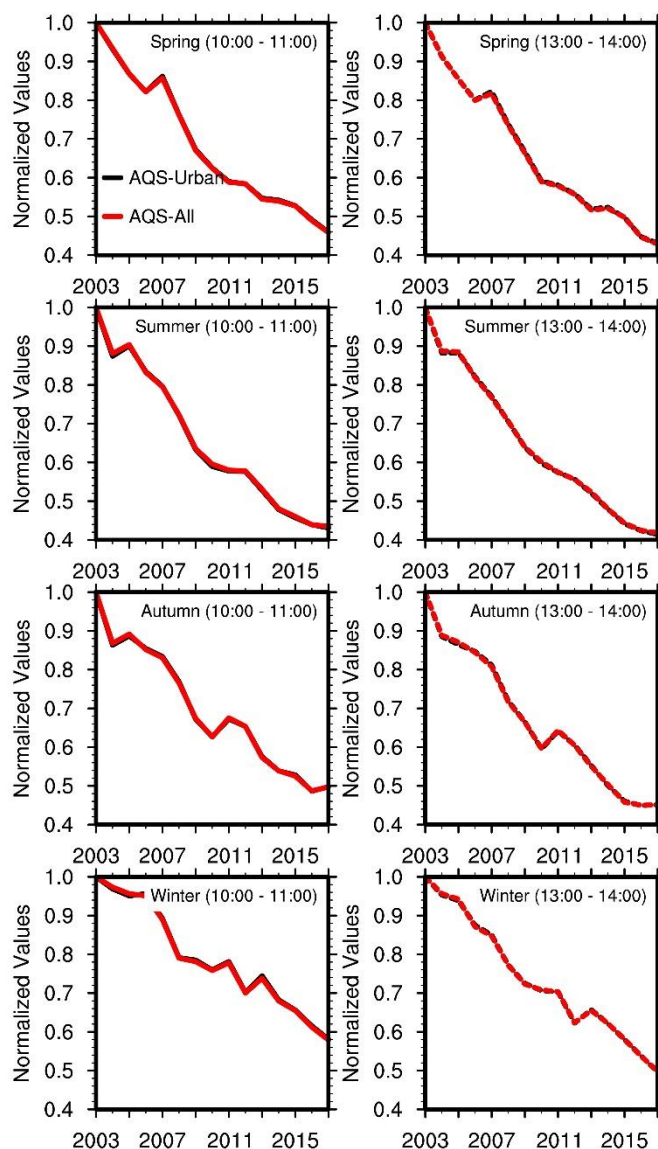


Figure R4. Relative annual variations of mean NO₂ surface concentrations from AQS sites. Black lines denote mean concentrations for only AQS urban sites, while red lines are for all AQS sites, including both rural and urban. The mean NO₂ concentrations are scaled by the corresponding 2003 values. The left column is for NO₂ concentrations at 10:00 – 11:00 LT, and the right column is for 13:00 – 14:00 LT.

l. 349-350 the sentence "They also identified model biases (...) natural emissions" is unclear, please either elaborate or delete.

Reply:

Silvern et al. (2019) shown that GEOS-Chem v11-02c underestimated NO₂ concentrations in the free troposphere compared to aircraft observations and satellite cloud-slicing results, which they thought was the reason why GEOS-Chem simulation results couldn't capture satellite NO₂ TVCD trends. We changed “natural emissions” to “missing natural emissions in the free troposphere” in Line 379 in the main manuscript.

- l. 378-381 The nonlinear relationship of NO_x with NO₂ TVCD is important, but so are the effects of properly accounting for the background. The fact that spaceborne instruments have a low sensitivity close to the surface (i.e. the averaging kernels) is also important and deserves to be mentioned in this discussion.

Reply:

Thank you for the suggestion. In this study, when we talk about nonlinearity (β and γ), we always mean any chemical and physical processes affecting the NO₂ TVCD and NO₂ surface concentrations, such as soil NO_x in the boundary layer and lightning NO_x in the free troposphere, chemistry, transport effect, and wet-dry depositions. We added other nonlinear factors in Lines 204 – 205 in the revised manuscript to make it clear. In Section 3.1, as mentioned above, now we have more discussion about the contributions of different factors to β and γ values. The low sensitivity of satellite sensors to the surface NO_x indeed emphasizes the selection of urban regions in inferring anthropogenic NO_x emissions from satellite datasets with more NO_x in the lower atmosphere compared to free troposphere to make the satellite signal meaningful to anthropogenic NO_x

emissions, but it is more related to the satellite measurement uncertainties which we have talked about in Lines 152 – 154 in the revised manuscript. We recommend reading Silvern et al. (2019) for more details about the vertical sensitivity of satellite sensors to NO₂ distributions.

Technical comments:

- in the title, "tend" should be "trend"

Reply:

Thanks. We corrected it.

- abstract line 15, add the word "bottom-up" (or "estimated") before "anthropogenic"

Reply:

The results shown in Lines 14 – 19 are based on the 1-month REAM simulation, where we indeed used the bottom-up NEI2011 emission inventory. However, the conclusions are widely applicable and not limited to NEI2011 or any other bottom-up emission inventories.

- l. 89 "mechanistic" (not "mechanical")

Reply:

Thanks. We corrected it. Please see Line 90 in the revised manuscript.

- l. 107 replace "measurements" by "sensors"

Reply:

We corrected it. Please see Line 117 in the revised manuscript.

- l. 109 add "instrument" after "SCIAMACHY"

Reply:

We added it. Please see Line 120 in the revised manuscript.

- l. 116 "These instruments measure transmitted, backscattered, and reflected radiation"
is unclear

Reply:

We changed it to a simple sentence "These instruments measure backscattered solar radiation). Please see Line 127 in the revised manuscript.

- l. 126 "OMINO2" (not OMNO2")

Reply:

NASA OMI NO₂ TVCD products are named as OMNO2. Please refer to
https://disc.gsfc.nasa.gov/datasets/OMNO2_V003/summary.

- l. 134 "choose" not "chose" (I guess)

Reply:

Thanks. We think it would be better to change "re-grid" to "re-gridded" in Line 145 in

the revised manuscript.

- l. 208 add *"the"* before *"model simulation"*

Reply:

Thanks. We added it. Please see Line 220 in the revised manuscript.

- l. 279 -280 *"sensitivities (...) to different anthropogenic NO_x emissions over the CONUS"* is confusing, please rephrase

Reply:

Yes. We changed it to “We further investigate OMI-QA4ECV NO₂ TVCD relative annual variations from 2005 - 2017 over the regions with different anthropogenic NO_x emissions in Figure 5.” Please see Lines 305 – 307 in the revised manuscript.

- l. 325 insert *"the"* before *"decreasing rates"*

Reply:

Thanks. We added it. Please see Line 353 in the revised manuscript.

- *References : use journal abbreviations, e.g. Atmos. Environ., etc.*

Reply:

Yes, we corrected it.

- *caption of Figure 5, line 672: specify the year (and month?) of the anthropogenic*

emissions used to define the groups

Reply:

Yes, we added it. Please see Line 705 in the revised manuscript.

References

- Beirle, S., Platt, U., Wenig, M., and Wagner, T.: Weekly cycle of NO₂ by GOME measurements: A signature of anthropogenic sources, *Atmos. Chem. Phys.*, 3, 2225-2232, 10.5194/acp-3-2225-2003, 2003.
- Boersma, K. F., Jacob, D. J., Trainic, M., Rudich, Y., De Smedt, I., Dirksen, R., and Eskes, H. J.: Validation of urban NO₂ concentrations and their diurnal and seasonal variations observed from the SCIAMACHY and OMI sensors using in situ surface measurements in Israeli cities, *Atmos. Chem. Phys.*, 9, 3867-3879, 10.5194/acp-9-3867-2009, 2009.
- Choi, Y., Kim, H., Tong, D., and Lee, P.: Summertime weekly cycles of observed and modeled NO_x and O₃ concentrations as a function of satellite-derived ozone production sensitivity and land use types over the Continental United States, *Atmos. Chem. Phys.*, 12, 6291-6307, 10.5194/acp-12-6291-2012, 2012.
- DenBleyker, A., Morris, R. E., Lindhjem, C. E., Parker, L. K., Shah, T., Koo, B., Loomis, C., and Dilly, J.: Temporal and Spatial Detail in Mobile Source Emission Inventories for Regional Air Quality Modeling, 2012 International Emission Inventory Conference, Florida, U.S., August 13 - 16, 2012, 2012.
- EPA: 2014 National Emissions Inventory, version 2 - Technical Support Document, Research Triangle Park, North Carolina, 414, 2018.
- Herman, J., Cede, A., Spinei, E., Mount, G., Tzortziou, M., and Abuhassan, N.: NO₂ column amounts from ground-based Pandora and MFDOAS spectrometers using the direct-Sun DOAS technique: Intercomparisons and application to OMI validation, *J. Geophys. Res.-Atmos.*, 114, 10.1029/2009JD011848, 2009.
- Jiang, Z., McDonald, B. C., Worden, H., Worden, J. R., Miyazaki, K., Qu, Z., Henze, D. K., Jones, D. B. A., Arellano, A. F., and Fischer, E. V.: Unexpected slowdown of US pollutant emission reduction in the past decade, *Proc. Natl. Acad. Sci. U.S.A.*, 201801191, 10.1073/pnas.1801191115, 2018.
- Judd, L. M., Al-Saadi, J. A., Valin, L. C., Pierce, R. B., Yang, K., Janz, S. J., Kowalewski, M. G., Szykman, J. J., Tiefengraber, M., and Mueller, M.: The Dawn of Geostationary Air Quality Monitoring: Case Studies from Seoul and Los Angeles, *Front. Environ. Sci.*, 6, 85, 10.3389/fenvs.2018.00085, 2018.
- Kaynak, B., Hu, Y., Martin, R. V., Sioris, C. E., and Russell, A. G.: Comparison of weekly cycle of NO₂ satellite retrievals and NO_x emission inventories for the continental United States, *J. Geophys. Res.-Atmos.*, 114, 10.1029/2008JD010714, 2009.
- Kim, S. W., McDonald, B., Baidar, S., Brown, S., Dube, B., Ferrare, R., Frost, G., Harley, R., Holloway, J., and Lee, H. J.: Modeling the weekly cycle of NO_x and CO emissions and their impacts on O₃ in the Los Angeles-South Coast Air Basin during the CalNex 2010 field campaign, *J. Geophys. Res.-Atmos.*, 121, 1340-1360, 10.1002/2015JD024292, 2016.

Lamsal, L. N., Martin, R. V., Padmanabhan, A., Van Donkelaar, A., Zhang, Q., Sioris, C. E., Chance, K., Kurosu, T. P., and Newchurch, M. J.: Application of satellite observations for timely updates to global anthropogenic NO_x emission inventories, *Geophys. Res. Lett.*, 38, 10.1029/2010GL046476, 2011.

Lamsal, L. N., Duncan, B. N., Yoshida, Y., Krotkov, N. A., Pickering, K. E., Streets, D. G., and Lu, Z.: US NO₂ trends (2005–2013): EPA Air Quality System (AQS) data versus improved observations from the Ozone Monitoring Instrument (OMI), *Atmos. Environ.*, 110, 130-143, 10.1016/j.atmosenv.2015.03.055, 2015.

Seinfeld, J. H., and Pandis, S. N.: *Atmospheric chemistry and physics: from air pollution to climate change*, John Wiley & Sons, Inc, Hoboken, New Jersey, 2016.

Silvern, R. F., Jacob, D. J., Mickley, L. J., Sulprizio, M. P., Travis, K. R., Marais, E. A., Cohen, R. C., Laughner, J. L., Choi, S., Joiner, J., and Lamsal, L. N.: Using satellite observations of tropospheric NO₂ columns to infer long-term trends in US NO_x emissions: the importance of accounting for the free tropospheric NO₂ background, *Atmos. Chem. Phys.*, 19, 8863-8878, 10.5194/acp-19-8863-2019, 2019.

Response to Aristeidis Georgoulas

Thank you for your useful suggestions. Our answers follow your comments (in *Italics*).

Comments/suggestions:

Dear authors, in support of your results I would like to bring your attention to a recent study on satellite-based tropospheric NO₂ trends and trend reversals (1996-2017). In this study, it is shown that several regions in the US experienced a trend reversal around the period 2000 from positive or neutral trends to negative ones. There are also results for selected megacities in the US (e.g. Los Angeles).

Georgoulas, A. K., van der A, R. J., Stammes, P., Boersma, K. F., and Eskes, H. J.:

Trends and trend reversal detection in 2 decades of tropospheric NO₂ satellite observations, Atmos. Chem. Phys., 19, 6269-6294, <https://doi.org/10.5194/acp-19-6269-2019>, 2019.

Reply:

Thank you for providing a useful reference. We cited the paper in Line 46 in the revised manuscript.

Other changes

We found a bug in the calculation of β and γ , and thus updated Figure 2. The update has no effect on the trend analyses in the manuscript except for updating β and γ values in Table 2 (Lines 667 – 669) and on Line 364 in the revised manuscript. For urban regions, β and γ values are very close to before.

- 1
- 2
- 3
- 4
- 5
- 6
- 7
- 8
- 9
- 10

5

6
7

8

9

10

Abstract

We illustrate the nonlinear relationships among anthropogenic NO_x emissions, NO₂ tropospheric vertical column densities (TVCDs), and NO₂ surface concentrations using model simulations for July 2011 over the contiguous United States (CONUS). The variations of NO₂ surface concentrations and TVCDs are generally consistent and reflect well anthropogenic NO_x emission variations for high-anthropogenic-NO_x emission regions. For low-anthropogenic-NO_x emission regions, however, nonlinearity in the emission-TVCD relationship due to emissions from lightning and soils, chemistry, and physical processes makes it difficult to use satellite observations to infer anthropogenic NO_x emission changes. The analysis is extended to 2003 – 2017. Similar variations of NO₂ surface measurements and coincident satellite NO₂ TVCDs over urban regions are in sharp contrast to the large variation differences between surface and satellite observations over rural regions. We find a continuous decrease of anthropogenic NO_x emissions after 2011 by examining surface and satellite measurements in CONUS urban regions, but the decreasing rate is lower by 9% - 46% than the pre-2011 period.

1. Introduction

Anthropogenic emissions of nitrogen oxides ($\text{NO}_x = \text{NO}_2 + \text{NO}$) adversely affect the environment, not only because of their direct detrimental impacts on human health (Greenberg et al., 2016; Greenberg et al., 2017; Heinrich et al., 2013; Weinmayr et al., 2009), but also their fundamental roles in the formation of ozone, acid rain, and fine particles which are unfavorable to human health, ecosystem stabilities, and climate change (Crouse et al., 2015; Kampa and Castanas, 2008; Myhre et al., 2013; Pandey et al., 2005; Singh and Agrawal, 2007). About 48.8 Tg N yr^{-1} of NO_x are emitted globally from both anthropogenic (77%) and natural (23%) sources, such as fossil fuel combustion, biomass and biofuel burning, soil bacteria, and lightning (Seinfeld and Pandis, 2016). 3.85 Tg N and 0.24 Tg N of anthropogenic and ~~natural-soil~~ NO_x , respectively, were emitted from the U.S. in 2014 on the basis of the 2014 National Emission Inventory (NEI2014); vehicle sources and fuel combustions accounted for 93% of the total anthropogenic NO_x emissions (EPA, 2017).

The U.S. anthropogenic NO_x emissions during the 2010s declined dramatically compared to the mid-2000s (EPA, 2018; Xing et al., 2013) due to stricter air quality regulations and emission control technology improvements, such as the phase-in of Tier II vehicles during 2004 – 2009 and the switch of power plants from coal to natural gas (De Gouw et al., 2014; McDonald et al., 2018). The overall reduction (about 30% - 50%) of anthropogenic NO_x emissions from the mid-2000s to the 2010s was corroborated by observed decreasing of vehicle NO_x emission factors, NO_2 surface concentrations, nitrate wet deposition flux (Figure S1), and NO_2 tropospheric vertical column densities (TVCDs) (Bishop and Stedman, 2015; Georgoulas et al., 2019; Li et al., 2018; McDonald et al., 2018; Miyazaki et al., 2017; Russell et al., 2012; Tong et al., 2015). However, the detailed NO_x emission changes after the Great Recession (from December 2007 to June 2009) are highly uncertain. On the one hand, the U.S. Environmental Protection Agency

(EPA) estimated that the Great Recession had a slight impact on the anthropogenic NO_x emission trend, and the anthropogenic NO_x emissions decreased steadily from 2002 to 2017 (Figure S24), although the emission decrease rate slowed down by about 20% after 2010 (-5.8% yr⁻¹ for 2002 – 2010, and -4.7% yr⁻¹ for 2010 – 2017, Table 1) (EPA, 2018). Fuel-based emission estimates in Los Angeles also showed a steady decrease of anthropogenic NO_x emissions after 2000 and a small impact of the Great Recession on anthropogenic NO_x emission decrease trend (Hassler et al., 2016). The continuous decrease of anthropogenic NO_x emissions was consistent with the ongoing reduction of vehicle emissions (McDonald et al., 2018). On the other hand, Miyazaki et al. (2017) and Jiang et al. (2018) found that the U.S. NO_x emissions derived from satellite NO₂ TVCDs, including OMI (the Ozone Monitoring Instrument), SCIAMACHY (SCanning Imaging Absorption SpectroMeter for Atmospheric CHartography), and GOME-2A (Global Ozone Monitoring Experiment – 2 onboard METOP-A), were almost flat from 2010 - 2015 and suggested that the decrease of NO_x emissions was only significant before 2010, which was completely different from the bottom-up and fuel-based emission estimates.

A complicating factor in inferring anthropogenic NO_x emission trends from the observations of NO₂ surface concentrations and satellite NO₂ TVCDs is the nonlinearity in NO_x chemistry (Gu et al., 2013; Gu et al., 2016; Lamsal et al., 2011). Although the decrease rates of both NO₂ surface concentrations and coincident OMI NO₂ TVCDs slowed down after the Great Recession over the United States, Tong et al. (2015), Lamsal et al. (2015) and Jiang et al. (2018) found that the slowdown of the decrease rates derived from NO₂ surface concentrations is 12% - 79% less than those of NO₂ TVCDs (Table 1). Secondly, the slowdown of the decrease rates of NO₂ surface concentrations and OMI TVCDs over cities and power plants (Russell et al., 2012; Tong et al., 2015) is significantly less than those over the whole contiguous United States (CONUS) (Jiang et al., 2018; Lamsal et al., 2015). Moreover, Zhang et al. (2018) found that filtering out lightning-

affected measurements could significantly improve the comparison of NO₂ surface concentration and OMI NO₂ TVCD trends over the CONUS.

In this study, we carefully investigate the relationships among anthropogenic NO_x emissions, NO₂ surface concentrations, and NO₂ TVCDs over the CONUS and evaluate the impact of the relationships on inferring anthropogenic NO_x emission changes and trends from surface and satellite observations. Section 2 describes the model and datasets used in this study, including the Regional chemistry and transport Model (REAM), the EPA Air Quality System (AQS) NO₂ surface observations, and NO₂ TVCD products from OMI, GOME-2A, GOME-2B (GOME2 onboard METOP-B), and SCIAMACHY. In Section 3, we examine the nonlinear relationships among anthropogenic NO_x emissions, NO₂ surface concentrations, and NO₂ TVCDs using model simulations. Accounting for the effects of chemical nonlinearity, we then investigate the anthropogenic NO_x emission trends and changes from 2003 – 2017 over the CONUS. Finally, section 4 gives a summary of the study.

2. Model and Data Description

2.1 REAM

The REAM model has been applied and evaluated in many research applications including ozone simulation and forecast, emission inversion and evaluations, and ~~mechanical~~mechanistic studies of chemical and physical processes (Alkuwari et al., 2013; Cheng et al., 2017; Cheng et al., 2018; Choi et al., 2008a; Choi et al., 2008b; Gu et al., 2013; Gu et al., 2014; Koo et al., 2012; Liu et al., 2012; Liu et al., 2014; Wang et al., 2007; Yang et al., 2011; Zhang et al., 2017; Zhang et al., 2018; Zhang and Wang, 2016; Zhao and Wang, 2009; Zhao et al., 2009a; Zhao et al., 2010). REAM used in this work, the model domain of which is shown in Figure 3, has 30 vertical layers in the troposphere, and the horizontal resolution is 36 × 36 km². The model is driven by

meteorology fields from a Weather and Research Forecasting (WRF, version 3.6) model
 simulation initialized and constrained by the NCEP coupled forecast system model version 2
 (CFSv2) products (Saha et al., 2011). The chemistry mechanism is based on GEOS-Chem v11.01
 with updated reaction rates and aerosol uptake of isoprene nitrates (Fisher et al., 2016). Chemistry
 boundary conditions and initializations are from a GEOS-Chem ($2^\circ \times 2.5^\circ$) simulation. Hourly
 anthropogenic emissions on weekdays are based on the 2011 National Emission Inventory
 (NEI2011), while weekend anthropogenic emissions are set to be two-thirds of the weekday
 emissions (Beirle et al., 2003; Choi et al., 2012). Biogenic VOC emissions are estimated using the
 Model of Emissions of Gases and Aerosols from Nature (MEGAN) v2.10 (Guenther et al., 2012).
 NO_x emissions from soils are based on the Yienger and Levy (YL) scheme (Li et al., 2019;
 Yienger and Levy, 1995). The cloud-to-ground (CG) lightning flashes are calculated following
Choi et al. (2005) and Zhao et al. (2009a) with the parameterization of CG flash rate as a function
of convective mass fluxes and convective available potential energy (CAPE). The ratios of intra-
cloud (IC) lightning flashes to CG flashes are parameterized as a function of the height between
the freezing layer and the cloud top (Luo et al., 2017; Price and Rind, 1992). In this study, 250
moles of NO are emitted per CG or IC flash (Zhao et al., 2009a). As a result, on weekdays in July
2011, REAM has mean anthropogenic NO_x emissions of 7.4×10^{10} molecules cm⁻² s⁻¹, mean soil
NO_x emissions of 1.2×10^{10} molecules cm⁻² s⁻¹, and mean lightning NO_x emissions of 3.4×10^{10}
molecules cm⁻² s⁻¹ over the CONUS.

2.2 Satellite NO₂ TVCDs

In this study, we use NO₂ TVCD products from four satellite ~~measurements-sensors~~ in the
 past decade, including SCIAMACHY, GOME-2A, GOME-2B, and OMI, the spectrometers
 onboard sun-synchronous satellites to monitor atmospheric trace gases. The SCIAMACHY
~~instrument~~ onboard the Environmental Satellite (ENVISAT) has an equator overpass time of
 10:00 Local time (LT) and a nadir pixel resolution of 60×30 km². The GOME-2 instruments on

Metop-A (named as GOME-2A) and Metop-B (GOME-2B) satellites cross the equator at 9:30 LT and have a nadir resolution of $80 \times 40 \text{ km}^2$. After July 15, 2013, the nadir resolution of GOME-2A became $40 \times 40 \text{ km}^2$ with a smaller scanning swath. The OMI onboard the EOS-Aura satellite has a nadir resolution of $24 \times 13 \text{ km}^2$ and overpasses the equator around 13:45 LT. More detailed information about these instruments is summarized in Table S1. These instruments measure ~~transmitted, backscattered, and reflected~~ solar radiation from the atmosphere in the ultraviolet and visible wavelength. The radiation measurements in the wavelength of 402 - 465 nm are then used to retrieve NO_2 VCDs. The retrieval process consists of three steps: 1) converting radiation observations to NO_2 slant column densities (SCDs) by using the Differential Optical Absorption Spectroscopy (DOAS) spectral fitting method; 2) separating tropospheric SCDs and stratospheric SCDs from the total NO_2 SCDs; 3) dividing the NO_2 tropospheric SCDs by the tropospheric air mass factors (AMF) to compute VCDs.

The product archives we use in this study include GOME-2B (TM4NO2A v2.3), SCIAMACHY (QA4ECV v1.1), GOME-2A (QA4ECV v1.1), OMI (QA4ECV v1.1, hereafter referred to as OMI-QA4ECV), OMNO2 (SPv3, hereafter referred to as OMI-NASA), and the Berkeley High-Resolution NO_2 products (v3.0B, hereafter referred to as OMI-BEHR). OMI-BEHR uses the tropospheric SCDs from OMI-NASA products but updates some inputs for the tropospheric AMF calculation (Laughner et al., 2018). These product archives have been previously validated (Boersma et al., 2018; Drosoglou et al., 2017; Drosoglou et al., 2018; Krotkov et al., 2017; Laughner et al., 2018; Wang et al., 2017; Zara et al., 2018). Generally, the pixel-size uncertainties of these products are $> 30\%$ over polluted regions under clear-sky conditions. We summarize the basic information about these products in Table S2. To keep the high quality and sampling consistency of NO_2 TVCD datasets, we chose pixel-size NO_2 TVCD data using the criteria listed in Table S3. After the selection, we re-grid~~ded~~ the pixel-size data into the REAM $36 \times 36 \text{ km}^2$ grid cells and calculate the seasonal means of each grid cell with

corresponding daily values on weekdays (winter: January, February, and December; spring: March, April, and May; summer: June, July, and Autumn; autumn: September, October, and November). We excluded weekend data in this study to minimize the impacts of weekend NO_x emission reduction, leading to different NO₂ TVCDs between weekdays and weekends (Figure S32).

Satellite TVCD measurements can show large variations and apparent discontinuities due in part to the effects of cloud, lightning NO_x, the shift of satellite pixel coverage, and retrieval uncertainties (Figure S32; e.g., (Boersma et al., 2018; Zhang et al., 2018)). However, continuous and consistent measurements are required for reliable trend analyses. In addition to the criteria of data selection in Table S3, we compute the seasonal relative 90th percentile confidence interval, defined as $RCI = (X(95^{th} \text{ percentile}) - X(5^{th} \text{ percentile})) / \text{mean}(X)$, where X is the daily NO₂ TVCD for a given season. To compute the seasonal trend, we require that RCI is < 50% for the selected season every year in the analysis period (Table S3). About 45% of data are removed as a result.

2.3 Surface NO₂ measurements

Hourly surface NO₂ measurements from 2003 - 2017 are from the EPA AQS monitoring network (archived on <https://www.epa.gov/outdoor-air-quality-data>). Most AQS monitoring sites use the Federal Reference Method (FRM) — gas-phase chemiluminescence to measure NO₂. Few sites use the Federal Equivalent Method (FEM) – photolytic-chemiluminescence or the Cavity Attenuated Phase Shift Spectroscopy (CAPS) method. FRM and FEM are indirect methods, in which NO₂ is first converted to NO and then NO is measured through chemiluminescence measurement of NO₂* produced by NO + O₃. The difference is that FRM uses heated reducers/catalysts for the conversion of NO₂ to NO and FEM uses photolysis of NO₂ to NO. The conversion to NO in the FRM instruments is not specific to NO₂, and non-NO_x active nitrogen

compounds (NO_z) can also be reduced by the catalysts, which would cause high biases of NO_2 measurements, while the FEM method is sensitive to the photolysis conversion efficiency of NO_2 to NO (Beaver et al., 2012; Beaver et al., 2013; Lamsal et al., 2015). The CAPS method directly determines NO_2 concentrations based on a NO_2 -induced phase shift measured by a photodetector. The CAPS instrument operates at a wavelength of about 450 nm and may overestimate NO_2 concentrations due to absorption of other molecules at the same wavelength (Beaver et al., 2012; Beaver et al., 2013; Kebabian et al., 2005).

Due to the different characteristics of the above three methods and demonstrated biases between the FRM and the FEM by Lamsal et al. (2015), we firstly investigate the measurement discrepancies among the above three methods. There are three sites having FRM and FEM measurements simultaneously during some periods from 2013 - 2014, two sites having both FRM and CAPS data during some periods from 2015 – 2016, and one site using all three measurement methods during some periods in 2015. Figure S43 shows the hourly averaged ratios of FEM and CAPS to FRM data, respectively, for 4 seasons during 2013 – 2016. The CAPS/FRM ratios are in the range of 0.94 – 1.06 and the FEM/FRM ratios of 0.86 – 1.11. Furthermore, Zhang et al. (2018) discussed that the relative trends are not affected by scaling the observation data. As in the work by Zhang et al. (2018), we analyze the relative trends in the surface NO_2 data. We, therefore, did not scale the FRM data. At sites with FEM or CAPS measurements, we use these measurements in place of FRM data. If both FEM and CAPS data are available, we use the averages of the two datasets.

Since NO_2 surface concentrations have significant diurnal variations (Figure S54), we choose the data at 9:00-10:00 LT for comparison with GOME-2A/2B data, 10:00-11:00 LT for comparison with SCIAMACHY data, and 13:00-14:00 LT for OMI data. The seasonal $RCI < 50\%$ requirement is also used here to be consistent with the analysis of satellite TVCD data, and thus about 1.5% of the data are removed. We also require that the measurement site must have

valid measurements in the aforementioned 3 hours for at least one season from 2003 – 2017. The locations of the 179 selected sites using the site selection criteria are shown in Figure 1. The region definitions follow the U.S. Census Bureau (https://www2.census.gov/geo/pdfs/maps-data/maps/reference/us_regdiv.pdf).

3. Results and Discussions

3.1 Nonlinear relationships among anthropogenic NO_x emissions, NO₂ surface concentrations, and NO₂ TVCDs

NO₂ surface concentrations and NO₂ TVCD are not linearly correlated with NO_x emissions due in part to chemical nonlinearity, [wet and dry depositions, transport effects, background sources](#) (Gu et al., 2013; Lamsal et al., 2011). Therefore, it is necessary to first investigate the nonlinearities among NO_x emissions, NO₂ surface concentrations, and TVCDs over the CONUS before we compare the trends between NO₂ surface concentrations and TVCDs. The nonlinearity between NO_x emission and NO₂ TVCD is analyzed by examining the local sensitivity of NO₂ TVCD to NO_x emissions (Gu et al., 2013; Lamsal et al., 2011; Tong et al., 2015), which is defined as β in Equation (1). We further define γ as the sensitivity of NO₂ surface concentration to NO_x emission:

$$\frac{\Delta E}{E} = \beta \frac{\Delta \Omega}{\Omega} \quad (1)$$

$$\frac{\Delta E}{E} = \gamma \frac{\Delta c}{c} \quad (2)$$

where E denotes NO_x emission and ΔE denotes the change of NO_x emission; Ω denotes NO₂ TVCD, c denotes surface NO₂ concentration, and $\Delta \Omega$ and Δc denote the corresponding changes.

We computed β and γ values for July 2011 over the CONUS using REAM. To compute local β and γ values, we added another independent group of chemistry species (“group 2”) in REAM in order to compute the standard and sensitivity simulations concurrently. The original chemical species in the model (“group 1”) were used in the standard simulation. For group 2 chemical species, anthropogenic NO_x emissions were reduced by 15%. In the model simulation, we first computed the advection of group 1 tracers. The horizontal tracer fluxes were therefore available. All influxes into a grid cell for group 2 tracer simulation were from group 1 tracer simulation; only outfluxes were computed using group 2 tracers. The outflux was one way in that nitrogen species were transported out but the transport did not affect adjacent grid cells because the influxes were from group 1 tracer simulation. Using this procedure, the effects of anthropogenic NO_x emission reduction were localized. The β and γ values were computed by the ratio of TVCD and surface concentration changes to 15% change of anthropogenic NO_x emissions, respectively.

Figure 2 shows the distributions of our β and γ ratios as a function of anthropogenic NO_x emissions for July 2011 over the CONUS. Results essentially the same as Figure 2 were obtained when a perturbation of 10% was used for anthropogenic NO_x emissions. Figure S6 shows the distributions of NO_2 TVCD fraction in the boundary layer at 13:00 – 14:00 LT and 10:00 – 11:00 LT, and the fraction of soil NO_x emissions in all surface sources (soil + anthropogenic) on weekdays for July 2011, respectively. In Figure S7, we analyzed the contributions of background sources and non-emission factors (transport, chemistry, and wet and dry depositions) to the nonlinear relationships (β and γ) among anthropogenic NO_x emissions, NO_2 surface concentrations, and NO_2 TVCDs. While the model simulation is for one summer month, several key points on the surface and column concentration sensitivities to anthropogenic NO_x emissions have implications for comparing the trends of AQS and satellite TVCD data. (1) Both β and γ values are negatively correlated with anthropogenic NO_x emissions due to chemical nonlinearity.

transport. and background NO_x contributions (Figures 2, S6, and S7) (Gu et al., 2016; Lamsal et al., 2011). It is consistent with the distribution of β as a function of NO_x emissions in China (Gu et al., 2013), although the β ratios for the US are generally larger than for China due primarily to different emission distributions of NO_x and VOCs and regional circulation patterns (Zhao et al., 2009b). (2) The uncertainties of β and γ values increase significantly as anthropogenic NO_x emissions decrease, which means regions with low anthropogenic NO_x emissions are more sensitive to environmental conditions, such as NO_x transport from nearby regions which may even produce negative β and γ values (Figures 2 and S7). (3) The value of γ is generally less than β , especially for low-anthropogenic-NO_x emission regions, which reflects the significant contribution of free tropospheric NO₂ to NO₂ TVCD but not to NO₂ surface concentrations (Figures 2, S6, and S7). (4) The variations of β and γ values in anthropogenic NO_x emission bins tend to be larger at 10:00 – 11:00 than at 13:00 – 14:00 LT, reflecting a stronger transport effect due to weaker chemical losses at 10:00 – 11:00 (Figure 2). (5) Both β and γ values are significantly less than 1 at 13:00 – 14:00 LT ($\beta = 0.74$ and $\gamma = 0.84$) when anthropogenic NO_x emissions are $> 4 \times 10^{12}$ molecules cm⁻² s⁻¹, but they are close to 1 at 10:00 – 11:00 LT ($\beta = 0.96$ and $\gamma = 1.02$), which reflect stronger chemistry nonlinearity at 13:00 – 14:00 than in the morning (Figure 2). (6) Both background sources and non-emission factors contribute much more to β and γ values in low-anthropogenic-NO_x emission regions than in high-anthropogenic-NO_x emission regions (Figure S7). (7) Generally, non-emission factors contribute more to β and γ values than background sources in low-anthropogenic-NO_x emission regions (Figures S7c and S7d) except for the first bin where background sources contribute more to β and γ values than non-emission factors at 10:00 – 11:00, which is partly caused by some grid cells with extremely low anthropogenic NO_x emissions, increasing the mean contributions of background sources in the first bin.

The largely varying β and γ values for anthropogenic NO_x emissions $< 10^{11}$ molecules $\text{cm}^{-2} \text{s}^{-1}$ imply that the trends derived from satellite TVCD data do not directly represent anthropogenic NO_x emissions and that the variations of TVCD data may not be comparable to the corresponding surface NO_2 concentrations. We define a region “urban” if anthropogenic NO_x emissions [from NEI2011](#) are $> 10^{11}$ molecules $\text{cm}^{-2} \text{s}^{-1}$. All the other regions are defined as “rural”. Figure 3 shows the distributions of anthropogenic NO_x emissions and urban and rural regions defined in this study. Such defined urban regions account for 69.8% of the total anthropogenic NO_x emissions over the CONUS, the trend of which is, therefore, representative of anthropogenic emission changes. A caveat is that some “urban” regions would become “rural” if anthropogenic NO_x emissions decreased after 2011 as the EPA anthropogenic NO_x emission trend suggested (Figure S24). In a sensitivity study, we define an urban region using a stricter criterion of anthropogenic NO_x emissions $> 2 \times 10^{11}$ molecules $\text{cm}^{-2} \text{s}^{-1}$ and the analysis results are similar to those shown in the next section.

3.2 Trend comparisons between NO_2 AQS surface concentrations and coincident satellite NO_2 tropospheric VCD over urban and rural regions

By using anthropogenic NO_x emissions of 10^{11} molecules $\text{cm}^{-2} \text{s}^{-1}$ as the threshold value, 157 AQS sites are urban, and the rest 22 sites are rural. Their properties are summarized in Table 2. Figure 4 shows the relative annual variations of AQS NO_2 surface measurements at 13:00 – 14:00 and coincident OMI-QA4ECV NO_2 TVCD data from 2005 – 2017 in each season for urban and rural regions. The contrast between the two regions is apparent in all seasons. For comparison purposes, we scale the time series of TVCD and AQS surface NO_2 to their corresponding 2005 values, and the resulting data are therefore unitless. Over urban regions, NO_2 surface concentrations are highly correlated with NO_2 TVCDs ($\text{TVCD} = 1.03 \times \text{AQS} + 0.11$, $R^2 = 0.98$), reflecting the comparable and stable β and γ values (Figure 2). However, over rural regions, the scaled TVCD data significantly deviate from AQS NO_2 data ($\text{TVCD} = 1.15 \times \text{AQS} + 0.09$, $R^2 =$

0.87). It is noteworthy that the discrepancies between urban and rural data are smaller in winter than in spring, summer, and autumn due to a more dominant role of transport than chemistry and lower natural NO_x emissions in winter.

We also examine the correlations of AQS NO₂ surface concentrations with coincident OMI-NASA, OMI-BEHR, SCIAMACHY, GOME-2A, and GOME-2B TVCD measurements. The results of OMI-NASA and OMI-BEHR are similar to those of OMI-QA4ECV (Figure 4). SCIAMACHY and GOME-2B TVCD observations at 9:00-11:00 LT also show large contrast between urban (SCIAMACHY: TVCD = $0.92 \times \text{AQS} - 0.005$, $R^2 = 0.94$; GOME-2B: TVCD = $0.54 \times \text{AQS} + 0.56$, $R^2 = 0.96$) and rural regions (SCIAMACHY: TVCD = $0.77 \times \text{AQS} + 0.83$, $R^2 = 0.63$; GOME-2B: TVCD = $0.46 \times \text{AQS} + 0.73$, $R^2 = 0.59$). The correlation of coincident GOME-2A NO₂ TVCD data with AQS surface concentrations is poor for rural (TVCD = $0.65 \times \text{AQS} + 0.56$, $R^2 = 0.44$) and urban (TVCD = $0.31 \times \text{AQS} + 0.56$, $R^2 = 0.21$) regions (Figure S85), which likely reflects the degradation of the GOME-2A instrument causing significant increase of NO₂ SCD uncertainties (Boersma et al., 2018). Therefore, we excluded GOME-2A in the analysis hereafter.

We further investigate ~~the sensitivities of~~ OMI-QA4ECV NO₂ TVCD relative annual variations from 2005 - 2017 over the regions with different anthropogenic NO_x emissions ~~over the CONUS~~ in Figure 5. We find clear flattening of NO₂ TVCD variations as anthropogenic NO_x emissions decrease, which is consistent with the above analysis. Similar to Figure 4, the spread of TVCD variation is much less in winter than the other seasons. The differences between Figures 5 and 4 are due to a much larger dataset used in the former than the latter. Only coincident AQS and OMI-QA4ECV data are used in Figure 4, but all OMI-KMNI data are used in Figure 5.

3.3 Trend analysis of AQS NO₂ surface concentrations, satellite TVCDs, and updated EPA NO_x emissions

We first updated the CEMS measurement data used in the EPA NO_x emission trend datasets with the newest datasets obtained from <https://ampd.epa.gov/ampd/>. As shown in Figure S24, the updated CEMS data lead to a reduction of anthropogenic NO_x emissions during the Great Recession (2008 – 2009) and a recovery period in 2010 – 2011. The sharp drop during the Great Recession and the flattening trend right after the Great Recession are captured by OMI NO₂ and SCIAMACHY TVCD products (Figures 4, 6, and S96) and AQS NO₂ surface measurements (Figures 4, 6, and S54) and are also noted by Russell et al. (2012) and Tong et al. (2015) (Table 1).

In Figure 6, we show the comparisons among the relative variations of the updated EPA anthropogenic NO_x emissions, AQS NO₂ surface measurements at 10:00-11:00 and 13:00-14:00, and coincident satellite NO₂ TVCDs for urban regions in 4 seasons from 2003 to 2017. Also shown are the comparisons among the updated EPA anthropogenic NO_x emissions and satellite NO₂ TVCDs. There are many more data points for the latter comparison because the data selection is no longer limited to those coincident with the AQS surface data, and therefore, the uncertainty spread is much lower. The comparisons, in general, show consistent results that the updated EPA anthropogenic NO_x emissions, AQS surface measurements, and satellite TVCD data are in agreement. The agreement of decreasing trends among the datasets is just as good for the post-2011 period as the pre-2011 period. This result differs from Miyazaki et al. (2017) and Jiang et al. (2018), who suggested no significant decreasing trend for OMI TVCD data and inversed NO_x emissions after 2010. The disagreement can be explained by the results of Figure 5. Including the low anthropogenic NO_x emission regions leads to underestimates of NO_x decreases. Since the area of low anthropogenic NO_x emission regions is larger than high anthropogenic NO_x emission regions (Table 2), the arithmetic averaging will lead to a large weighting of rural

observations, which do not reflect anthropogenic NO_x emission changes. Miyazaki et al. (2017) and Jiang et al. (2018) included all regions in their analyses, but we exclude rural regions. Figure S96 shows the seasonal variations if the TVCDs over rural regions are included; the result shows a much lower decreasing rate of TVCDs over the CONUS. The much slower satellite TVCD trends for regions with low NO_x emissions was previously discussed by Zhang et al. (2018). In addition, Miyazaki et al. (2017) and Jiang et al. (2018) conducted NO_x emission inversions by using the Model for Interdisciplinary Research on Climate (MIROC)-Chem with a coarse resolution of $2.8^{\circ} \times 2.8^{\circ}$, which was insufficient to separate urban and rural regions and might distort predicted NO₂ TVCDs and inversed NO_x emissions due to nonlinear effects (Valin et al., 2011; Yu et al., 2016), which is another possible reason for their find of flattening NO_x emission trends after 2010.

We summarize the decreasing rates of NO₂ after the Great Recession in Table 3. To minimize the effect of the sharp decrease and the subsequent recovery, we chose to analyze the post-2011 period. Table 3 summarizes the results for each season, while Table 1 gives the averaged annual decreasing trends. Generally, Tables 1 and 3 confirm the continuous decreases of AQS surface observations, satellite NO₂ TVCD, and updated EPA anthropogenic NO_x emissions after 2011 as in Figure 6, but the decreasing rates are lower than the pre-2011 period. Over the AQS urban sites, the slowdown magnitudes are 9% for AQS surface observations and 20% - 40% for satellite NO₂ TVCD measurements, which may reflect in part smaller γ than β values (Table 2). Our estimated slowdown magnitudes are significantly lower than Lamsal et al. (2015) and Jiang et al. (2018) ~~but comparable to the results by Tong et al. (2015)~~ (Table 1). ~~The agreement with Tong et al. (2015) is because we select urban AQS sites based on anthropogenic NO_x emissions and they chose eight large cities, while Lamsal et al. (2015) and Jiang et al. (2018) used all AQS sites, which might be caused by their different data processing methods, such as including AQS sites with incomplete measurement records~~ (Silvern et al., 2019).

Over the CONUS urban regions, updated EPA anthropogenic NO_x emissions show a slowdown of 22% compared to 29% - 46% for three OMI NO₂ TVCD products. The difference is partially due to the β ratio of 2.53 ± 1.00 at 13:00 – 14:00 over the CONUS urban regions (Table 2). Satellite NO₂ TVCD measurement uncertainties also contribute to the difference. From 2013 – 2017, GOME-2B NO₂ TVCDs decrease more than OMI products, especially in spring, autumn and winter (Tables 1 and 3). Finally, trend analyses in different regions (Figure 7 and Table S4) indicate that generally, the Midwest has the least slowdown of the decreasing rate for urban OMI NO₂ TVCD (-14% on average) after 2011 compared to the Northeast (-30%), South (-34%), and West (-28%).

The results presented in this study are qualitatively in agreement with the work by Silvern et al. (2019). The two studies were independent. Therefore, the foci of the studies are different despite reaching similar conclusions. While we focused on understanding the detailed data analysis of Jiang et al. (2018) and limited the use of model simulation results so that our results can be compared to the previous study directly, Silvern et al. (2019) relied more on multi-year model simulations. As a result, Silvern et al. (2019) can clearly identify the contributions of the NO₂ columns by natural emissions and make use of additional observations such as nitrate deposition fluxes. They also identified model biases in simulating the trends of NO₂ TVCDs by missing natural emissions in the free troposphere. Our study, on the other hand, explored the data analysis procedure through which the trend of anthropogenic emissions can be derived from satellite observations and its limitations.

4. Conclusions

Using model simulations for July 2017, we demonstrate the nonlinear relationship of NO₂ surface concentration and TVCD with anthropogenic NO_x emissions. Over low anthropogenic NO_x emission regions, the ratios of anthropogenic NO_x emission changes to the changes of

surface concentrations (γ) and TVCDs (β) have very large variations and $\beta > \gamma \gg 1$. Therefore, for the same emission changes, surface concentration and TVCD changes are much smaller and variable than urban regions, making it difficult to use the observations to directly infer anthropogenic NO_x emission trends. We find that defining urban regions where anthropogenic NO_x emissions are $> 10^{11}$ molecules $\text{cm}^{-2} \text{s}^{-1}$ and using surface and TVCD observations over these regions can infer the trends that can be compared with the EPA emission trend estimates.

We evaluate the anthropogenic NO_x emission variations from 2003 – 2017 over the CONUS by using satellite NO_2 TVCD products from GOME-2B, SCIAMACHY, OMI-QA4ECV, OMI-NASA, and OMI-BEHR, over the urban regions of CONUS. We find broad agreements among the decreases of AQS NO_2 surface observations, satellite NO_2 TVCD products, and the EPA anthropogenic NO_x emissions with the CEMS dataset updated. After 2011, they all show a slowdown of the decreasing rates. Over the AQS urban sites, NO_2 surface concentrations have a slowdown of 9% and OMI products show a slowdown of 20% - 40%. Over the CONUS urban regions, OMI TVCD products indicate a slowdown of 29% - 46%, and the updated EPA anthropogenic NO_x emissions have a slowdown of 22%. The different slowdown magnitudes between OMI TVCD products and the other two datasets may be caused by the nonlinear response of TVCD to anthropogenic emissions and the uncertainties of satellite measurements (e.g., GOME-2B TVCD data show a larger decreasing trend than OMI products from 2013 – 2017).

We did not find observation evidence supporting the notion that anthropogenic NO_x emissions have not been decreasing after the Great Recession. In future studies, we recommend that the nonlinear relationships of NO_x emissions with NO_2 TVCD and surface concentration be

carefully evaluated when applying satellite and surface measurements to infer the changes of anthropogenic NO_x emissions.

Data availability

The EPA AQS hourly surface NO₂ measurements are downloaded from https://aqs.epa.gov/aqsweb/airdata/download_files.html#Raw. QA4ECV 1.1 NO₂ VCD products (OMI-QA4ECV, GOME-2A, and SCIAMACHY) are from <http://temis.nl/qa4ecv/no2col/data/>. GOME-2B NO₂ VCD products are from <http://www.temis.nl/airpollution/no2col/no2colgome2b.php>. OMI-BEHR and OMI-NASA archives are from <http://behr.cchem.berkeley.edu/DownloadBEHRData.aspx>. REAM simulation results for this study are available upon request.

Author contribution

JL and YW designed the study. JL conducted model simulations and data analyses with discussions with YW. JL and YW wrote the manuscript.

Competing interests

The authors declare that they have no conflict of interest.

Acknowledgments

This work was supported by the NASA ACMAP Program. We thank Ruixiong Zhang for discussions with J. Li. Thank Benjamin Wells, Alison Eyth, Lee Tooty from EPA, the EPA MOVES team, Betty Carter from COORDINATING RESEARCH COUNCIL, INC., Brain McDonald from NOAA, and Zhe Jiang from University of Science and Technology of China for helping us an understanding of the NEI MOVES mobile source emissions.

430 **References**

- 431 Alkuwari, F. A., Guillas, S., and Wang, Y.: Statistical downscaling of an air quality model using
432 Fitted Empirical Orthogonal Functions, *Atmos. Environ.*, 81, 1-10,
433 10.1016/j.atmosenv.2013.08.031, 2013.
- 434 Beaver, M., Long, R., and Kronmiller, K.: Characterization and Development of Measurement
435 Methods for Ambient Nitrogen Dioxide (NO₂), National Air Quality Conference - Ambient Air
436 Monitoring 2012, Denver, CO, US, 2012.
- 437 Beaver, M., Kronmiller, K., Duvall, R., Kaushik, S., Morphy, T., King, P., and Long, R.: Direct
438 and Indirect Methods for the Measurement of Ambient Nitrogen Dioxide, AWMA Measurement
439 Technologies meeting, Sacramento, CA, US, 2013.
- 440 Beirle, S., Platt, U., Wenig, M., and Wagner, T.: Weekly cycle of NO₂ by GOME measurements:
441 A signature of anthropogenic sources, *Atmos. Chem. Phys.*, 3, 2225-2232, 10.5194/acp-3-2225-
442 2003, 2003.
- 443 Bishop, G. A., and Stedman, D. H.: Reactive nitrogen species emission trends in three light-
444 /medium-duty United States fleets, *Environ. Sci. Technol.*, 49, 11234-11240,
445 10.1021/acs.est.5b02392, 2015.
- 446 Boersma, K. F., Eskes, H. J., Richter, A., De Smedt, I., Lorente, A., Beirle, S., van Geffen, J. H.,
447 Zara, M., Peters, E., and Roozendael, M. V.: Improving algorithms and uncertainty estimates for
448 satellite NO₂ retrievals: results from the quality assurance for the essential climate variables
449 (QA4ECV) project, *Atmos. Meas. Tech.*, 11, 6651-6678, 10.5194/amt-11-6651-2018, 2018.
- 450 Cheng, Y., Wang, Y., Zhang, Y., Chen, G., Crawford, J. H., Kleb, M. M., Diskin, G. S., and
451 Weinheimer, A. J.: Large biogenic contribution to boundary layer O₃-CO regression slope in
452 summer, *Geophys. Res. Lett.*, 44, 7061-7068, 10.1002/2017GL074405, 2017.
- 453 Cheng, Y., Wang, Y., Zhang, Y., Crawford, J. H., Diskin, G. S., Weinheimer, A. J., and Fried, A.:
454 Estimator of surface ozone using formaldehyde and carbon monoxide concentrations over the
455 eastern United States in summer, *J. Geophys. Res.-Atmos.*, 123, 7642-7655,
456 10.1029/2018JD028452, 2018.
- 457 Choi, Y., Wang, Y., Zeng, T., Martin, R. V., Kurosu, T. P., and Chance, K.: Evidence of lightning
458 NO_x and convective transport of pollutants in satellite observations over North America,
459 *Geophys. Res. Lett.*, 32, 10.1029/2004GL021436, 2005.
- 460 Choi, Y., Wang, Y., Yang, Q., Cunnold, D., Zeng, T., Shim, C., Luo, M., Eldering, A., Bucsela,
461 E., and Gleason, J.: Spring to summer northward migration of high O₃ over the western North
462 Atlantic, *Geophys. Res. Lett.*, 35, 10.1029/2007GL032276, 2008a.
- 463 Choi, Y., Wang, Y., Zeng, T., Cunnold, D., Yang, E. S., Martin, R., Chance, K., Thouret, V., and
464 Edgerton, E.: Springtime transitions of NO₂, CO, and O₃ over North America: Model evaluation
465 and analysis, *J. Geophys. Res.-Atmos.*, 113, 10.1029/2007JD009632, 2008b.

466 Choi, Y., Kim, H., Tong, D., and Lee, P.: Summertime weekly cycles of observed and modeled
 467 NO_x and O₃ concentrations as a function of satellite-derived ozone production sensitivity and land
 468 use types over the Continental United States, *Atmos. Chem. Phys.*, 12, 6291-6307, 10.5194/acp-
 469 12-6291-2012, 2012.

470 Crouse, D. L., Peters, P. A., Hystad, P., Brook, J. R., van Donkelaar, A., Martin, R. V.,
 471 Villeneuve, P. J., Jerrett, M., Goldberg, M. S., and Pope III, C. A.: Ambient PM_{2.5}, O₃, and NO₂
 472 exposures and associations with mortality over 16 years of follow-up in the Canadian Census
 473 Health and Environment Cohort (CanCHEC), *Environ. Health Perspect.*, 123, 1180,
 474 10.1289/ehp.1409276, 2015.

475 De Gouw, J. A., Parrish, D. D., Frost, G. J., and Trainer, M.: Reduced emissions of CO₂, NO_x,
 476 and SO₂ from US power plants owing to switch from coal to natural gas with combined cycle
 477 technology, *Earth's Future*, 2, 75-82, 10.1002/2013EF000196, 2014.

478 Drosoglou, T., Bais, A. F., Zyrichidou, I., Kouremeti, N., Poupkou, A., Liora, N., Giannaros, C.,
 479 Koukouli, M. E., Balis, D., and Melas, D.: Comparisons of ground-based tropospheric NO₂
 480 MAX-DOAS measurements to satellite observations with the aid of an air quality model over the
 481 Thessaloniki area, Greece, *Atmos. Chem. Phys.*, 17, 5829-5849, 10.5194/acp-17-5829-2017,
 482 2017.

483 Drosoglou, T., Koukouli, M. E., Kouremeti, N., Bais, A. F., Zyrichidou, I., Balis, D., Xu, J., and
 484 Li, A.: MAX-DOAS NO₂ observations over Guangzhou, China; ground-based and satellite
 485 comparisons, *Atmos. Meas. Tech.*, 11, 2239-2255, 10.5194/amt-11-2239-2018, 2018.

486 EPA: PROFILE OF VERSION 1 OF THE 2014 NATIONAL EMISSIONS INVENTORY, U.S.
 487 Environmental Protection Agency, 2017.

488 Air Pollutant Emissions Trends Data: [https://www.epa.gov/air-emissions-inventories/air-](https://www.epa.gov/air-emissions-inventories/air-pollutant-emissions-trends-data)
 489 [pollutant-emissions-trends-data](https://www.epa.gov/air-emissions-inventories/air-pollutant-emissions-trends-data), 2018.

490 Fisher, J. A., Jacob, D. J., Travis, K. R., Kim, P. S., Marais, E. A., Chan Miller, C., Yu, K., Zhu,
 491 L., Yantosca, R. M., and Sulprizio, M. P.: Organic nitrate chemistry and its implications for
 492 nitrogen budgets in an isoprene-and monoterpene-rich atmosphere: constraints from aircraft
 493 (SEAC⁴RS) and ground-based (SOAS) observations in the Southeast US, *Atmos. Chem. Phys.*,
 494 16, 5969-5991, 10.5194/acp-16-5969-2016, 2016.

495 Georgoulas, A. K., van der A, R. J., Stammes, P., Boersma, K. F., and Eskes, H. J.: Trends and
 496 trend reversal detection in 2 decades of tropospheric NO₂ satellite observations, *Atmos. Chem.*
 497 *Phys.*, 19, 6269-6294, 10.5194/acp-19-6269-2019, 2019.

498 Greenberg, N., Carel, R. S., Derazne, E., Bibi, H., Shpriz, M., Tzur, D., and Portnov, B. A.:
 499 Different effects of long-term exposures to SO₂ and NO₂ air pollutants on asthma severity in
 500 young adults, *J. Toxicol. Environ. Health, A*, 79, 342-351, 10.1080/15287394.2016.1153548,
 501 2016.

502 Greenberg, N., Carel, R. S., Derazne, E., Tiktinsky, A., Tzur, D., and Portnov, B. A.: Modeling
 503 long-term effects attributed to nitrogen dioxide (NO₂) and sulfur dioxide (SO₂) exposure on
 504 asthma morbidity in a nationwide cohort in Israel, *J. Toxicol. Environ. Health, A*, 80, 326-337,
 505 10.1080/15287394.2017.1313800, 2017.

506 Gu, D., Wang, Y., Smeltzer, C., and Liu, Z.: Reduction in NO_x emission trends over China:
 507 Regional and seasonal variations, *Environ. Sci. Technol.*, 47, 12912-12919, 10.1021/es401727e,
 508 2013.

509 Gu, D., Wang, Y., Smeltzer, C., and Boersma, K. F.: Anthropogenic emissions of NO_x over
 510 China: Reconciling the difference of inverse modeling results using GOME-2 and OMI
 511 measurements, *J. Geophys. Res.-Atmos.*, 119, 7732-7740, 10.1002/2014JD021644, 2014.

512 Gu, D., Wang, Y., Yin, R., Zhang, Y., and Smeltzer, C.: Inverse modelling of NO_x emissions over
 513 eastern China: uncertainties due to chemical non-linearity, *Atmos. Meas. Tech.*, 9, 5193-5201,
 514 10.5194/amt-9-5193-2016, 2016.

515 Guenther, A. B., Jiang, X., Heald, C. L., Sakulyanontvittaya, T., Duhl, T., Emmons, L. K., and
 516 Wang, X.: The Model of Emissions of Gases and Aerosols from Nature version 2.1
 517 (MEGAN2.1): an extended and updated framework for modeling biogenic emissions, *Geosci.*
 518 *Model Dev.*, 5, 1471-1492, 10.5194/gmd-5-1471-2012, 2012.

519 Hassler, B., McDonald, B. C., Frost, G. J., Borbon, A., Carslaw, D. C., Civerolo, K., Granier, C.,
 520 Monks, P. S., Monks, S., and Parrish, D. D.: Analysis of long-term observations of NO_x and CO
 521 in megacities and application to constraining emissions inventories, *Geophys. Res. Lett.*, 43,
 522 9920-9930, 10.1002/2016GL069894, 2016.

523 Heinrich, J., Thiering, E., Rzehak, P., Krämer, U., Hochadel, M., Rauchfuss, K. M., Gehring, U.,
 524 and Wichmann, H.-E.: Long-term exposure to NO₂ and PM₁₀ and all-cause and cause-specific
 525 mortality in a prospective cohort of women, *Occup. Environ. Med.*, 70, 179-186, 10.1136/oemed-
 526 2012-100876, 2013.

527 Jiang, Z., McDonald, B. C., Worden, H., Worden, J. R., Miyazaki, K., Qu, Z., Henze, D. K.,
 528 Jones, D. B. A., Arellano, A. F., and Fischer, E. V.: Unexpected slowdown of US pollutant
 529 emission reduction in the past decade, *Proc. Natl. Acad. Sci. U.S.A.*, 201801191,
 530 10.1073/pnas.1801191115, 2018.

531 Kampa, M., and Castanas, E.: Human health effects of air pollution, *Environ. Pollut.*, 151, 362-
 532 367, 10.1016/j.envpol.2007.06.012, 2008.

533 Kebabian, P. L., Herndon, S. C., and Freedman, A.: Detection of nitrogen dioxide by cavity
 534 attenuated phase shift spectroscopy, *Anal. Chem.*, 77, 724-728, 10.1021/ac048715y, 2005.

535 Koo, J.-H., Wang, Y., Kurosu, T. P., Chance, K., Rozanov, A., Richter, A., Oltmans, S. J.,
 536 Thompson, A. M., Hair, J. W., and Fenn, M. A.: Characteristics of tropospheric ozone depletion
 537 events in the Arctic spring: analysis of the ARCTAS, ARCPAC, and ARCIONS measurements
 538 and satellite BrO observations, *Atmos. Chem. Phys.*, 12, 9909-9922, 10.5194/acp-12-9909-2012,
 539 2012.

540 Krotkov, N. A., Lamsal, L. N., Celarier, E. A., Swartz, W. H., Marchenko, S. V., Bucsela, E. J.,
 541 Chan, K. L., Wenig, M., and Zara, M.: The version 3 OMI NO₂ standard product, *Atmos. Meas.*
 542 *Tech.*, 10, 3133-3149, 10.5194/amt-10-3133-2017, 2017.

543 Lamsal, L. N., Martin, R. V., Padmanabhan, A., Van Donkelaar, A., Zhang, Q., Sioris, C. E.,
 544 Chance, K., Kurosu, T. P., and Newchurch, M. J.: Application of satellite observations for timely

545 updates to global anthropogenic NO_x emission inventories, *Geophys. Res. Lett.*, 38,
 546 10.1029/2010GL046476, 2011.

547 Lamsal, L. N., Duncan, B. N., Yoshida, Y., Krotkov, N. A., Pickering, K. E., Streets, D. G., and
 548 Lu, Z.: US NO₂ trends (2005–2013): EPA Air Quality System (AQS) data versus improved
 549 observations from the Ozone Monitoring Instrument (OMI), *Atmos. Environ.*, 110, 130-143,
 550 10.1016/j.atmosenv.2015.03.055, 2015.

551 Laughner, J. L., Zhu, Q., and Cohen, R. C.: The Berkeley High Resolution Tropospheric NO₂
 552 product, *Earth System Science Data*, 10, 2069-2095, 10.5194/essd-10-2069-2018, 2018.

553 Li, J., Mao, J., Fiore, A. M., Cohen, R. C., Crounse, J. D., Teng, A. P., Wennberg, P. O., Lee, B.
 554 H., Lopez-Hilfiker, F. D., and Thornton, J. A.: Decadal changes in summertime reactive oxidized
 555 nitrogen and surface ozone over the Southeast United States, *Atmos. Chem. Phys.*, 18, 2341-
 556 2361, 10.5194/acp-18-2341-2018, 2018.

557 Li, J., Wang, Y., and Qu, H.: Dependence of summertime surface ozone on NO_x and VOC
 558 emissions over the United States: Peak time and value, *Geophys. Res. Lett.*, 46, 3540-3550,
 559 10.1029/2018GL081823, 2019.

560 Liu, Z., Wang, Y., Vrekoussis, M., Richter, A., Wittrock, F., Burrows, J. P., Shao, M., Chang, C.
 561 C., Liu, S. C., and Wang, H.: Exploring the missing source of glyoxal (CHOCHO) over China,
 562 *Geophys. Res. Lett.*, 39, 10.1029/2012GL051645, 2012.

563 Liu, Z., Wang, Y., Costabile, F., Amoroso, A., Zhao, C., Huey, L. G., Stickel, R., Liao, J., and
 564 Zhu, T.: Evidence of aerosols as a media for rapid daytime HONO production over China,
 565 *Environ. Sci. Technol.*, 48, 14386-14391, 10.1021/es504163z, 2014.

566 Luo, C., Wang, Y., and Koshak, W. J.: Development of a self-consistent lightning NO_x
 567 simulation in large-scale 3-D models, *J. Geophys. Res.-Atmos.*, 122, 3141-3154,
 568 10.1002/2016JD026225, 2017.

569 McDonald, B., McKeen, S., Cui, Y. Y., Ahmadov, R., Kim, S.-W., Frost, G. J., Pollack, I.,
 570 Peischl, J., Ryerson, T. B., and Holloway, J.: Modeling Ozone in the Eastern US using a Fuel-
 571 Based Mobile Source Emissions Inventory, *Environ. Sci. Technol.*, 10.1021/acs.est.8b00778,
 572 2018.

573 Miyazaki, K., Eskes, H., Sudo, K., Boersma, K. F., Bowman, K., and Kanaya, Y.: Decadal
 574 changes in global surface NO_x emissions from multi-constituent satellite data assimilation,
 575 *Atmos. Chem. Phys.*, 17, 807-837, 10.5194/acp-17-807-2017, 2017.

576 Myhre, G., Shindell, D., Bréon, F.-M., Collins, W., Fuglestad, J., Huang, J., Koch, D.,
 577 Lamarque, J.-F., Lee, D., Mendoza, B., Nakajima, T., Robock, A., Stephens, G., Takemura, T.,
 578 and Zhang, H.: Anthropogenic and natural radiative forcing, in: *Climate change 2013: The*
 579 *Physical Science Basis. Contribution of Working Group I to the Fifth Assessment Report of the*
 580 *Intergovernmental Panel on Climate Change*, Cambridge University Press, Cambridge, United
 581 Kingdom and New York, NY, USA, 659-740, 2013.

582 Pandey, J. S., Kumar, R., and Devotta, S.: Health risks of NO₂, SPM and SO₂ in Delhi (India),
 583 *Atmos. Environ.*, 39, 6868-6874, 10.1016/j.atmosenv.2005.08.004, 2005.

584 Price, C., and Rind, D.: A simple lightning parameterization for calculating global lightning
585 distributions, *J. Geophys. Res.-Atmos.*, 97, 9919-9933, 10.1029/92JD00719, 1992.

586 Russell, A. R., Valin, L. C., and Cohen, R. C.: Trends in OMI NO₂ observations over the United
587 States: effects of emission control technology and the economic recession, *Atmos. Chem. Phys.*,
588 12, 12197-12209, 10.5194/acp-12-12197-2012, 2012.

589 Seinfeld, J. H., and Pandis, S. N.: *Atmospheric chemistry and physics: from air pollution to*
590 *climate change*, John Wiley & Sons, Inc, Hoboken, New Jersey, 2016.

591 Silvern, R. F., Jacob, D. J., Mickley, L. J., Sulprizio, M. P., Travis, K. R., Marais, E. A., Cohen,
592 R. C., Laughner, J. L., Choi, S., Joiner, J., and Lamsal, L. N.: Using satellite observations of
593 tropospheric NO₂ columns to infer long-term trends in US NO_x emissions: the importance of
594 accounting for the free tropospheric NO₂ background, *Atmos. Chem. Phys.*, 19, 8863-8878,
595 10.5194/acp-19-8863-2019, 2019.

596 Singh, A., and Agrawal, M.: Acid rain and its ecological consequences, *J. Environ. Biol.*, 29, 15,
597 2007.

598 Tong, D., Lamsal, L., Pan, L., Ding, C., Kim, H., Lee, P., Chai, T., Pickering, K. E., and Stajner,
599 I.: Long-term NO_x trends over large cities in the United States during the great recession:
600 Comparison of satellite retrievals, ground observations, and emission inventories, *Atmos.*
601 *Environ.*, 107, 70-84, 10.1016/j.atmosenv.2015.01.035, 2015.

602 Valin, L. C., Russell, A. R., Hudman, R. C., and Cohen, R. C.: Effects of model resolution on the
603 interpretation of satellite NO₂ observations, *Atmos. Chem. Phys.*, 11, 11647-11655, 10.5194/acp-
604 11-11647-2011, 2011.

605 Wang, Y., Choi, Y., Zeng, T., Davis, D., Buhr, M., Huey, L. G., and Neff, W.: Assessing the
606 photochemical impact of snow NO_x emissions over Antarctica during ANTICI 2003, *Atmos.*
607 *Environ.*, 41, 3944-3958, 10.1016/j.atmosenv.2007.01.056, 2007.

608 Wang, Y., Beirle, S., Lampel, J., Koukouli, M., De Smedt, I., Theys, N., Ang, L., Wu, D., Xie, P.,
609 and Liu, C.: Validation of OMI, GOME-2A and GOME-2B tropospheric NO₂, SO₂ and HCHO
610 products using MAX-DOAS observations from 2011 to 2014 in Wuxi, China: investigation of the
611 effects of priori profiles and aerosols on the satellite products, *Atmos. Chem. Phys.*, 17, 5007,
612 10.5194/acp-17-5007-2017, 2017.

613 Weinmayr, G., Romeo, E., De Sario, M., Weiland, S. K., and Forastiere, F.: Short-term effects of
614 PM₁₀ and NO₂ on respiratory health among children with asthma or asthma-like symptoms: a
615 systematic review and meta-analysis, *Environ. Health Perspect.*, 118, 449-457,
616 10.1289/ehp.0900844, 2009.

617 Xing, J., Pleim, J., Mathur, R., Pouliot, G., Hogrefe, C., Gan, C. M., and Wei, C.: Historical
618 gaseous and primary aerosol emissions in the United States from 1990 to 2010, *Atmos. Chem.*
619 *Phys.*, 13, 7531-7549, 10.5194/acp-13-7531-2013, 2013.

620 Yang, Q., Wang, Y., Zhao, C., Liu, Z., Gustafson Jr, W. I., and Shao, M.: NO_x emission reduction
621 and its effects on ozone during the 2008 Olympic Games, *Environ. Sci. Technol.*, 45, 6404-6410,
622 10.1021/es200675v, 2011.

- 623 Yienger, J. J., and Levy, H.: Empirical model of global soil-biogenic NO_x emissions, *J. Geophys.*
624 *Res.-Atmos.*, 100, 11447-11464, 10.1029/95JD00370, 1995.
- 625 Yu, K., Jacob, D. J., Fisher, J. A., Kim, P. S., Marais, E. A., Miller, C. C., Travis, K. R., Zhu, L.,
626 Yantosca, R. M., and Sulprizio, M. P.: Sensitivity to grid resolution in the ability of a chemical
627 transport model to simulate observed oxidant chemistry under high-isoprene conditions, *Atmos.*
628 *Chem. Phys.*, 16, 4369-4378, 10.5194/acp-16-4369-2016, 2016.
- 629 Zara, M., Boersma, K. F., De Smedt, I., Richter, A., Peters, E., Van Geffen, J. H. G. M., Beirle,
630 S., Wagner, T., Van Roozendaal, M., and Marchenko, S.: Improved slant column density retrieval
631 of nitrogen dioxide and formaldehyde for OMI and GOME-2A from QA4ECV: intercomparison,
632 uncertainty characterization, and trends, *Meas. Tech. Discuss.*, 1-47, 10.5194/amt-11-4033-2018,
633 2018.
- 634 Zhang, R., Wang, Y., He, Q., Chen, L., Zhang, Y., Qu, H., Smeltzer, C., Li, J., Alvarado, L., and
635 Vrekoussis, M.: Enhanced trans-Himalaya pollution transport to the Tibetan Plateau by cut-off
636 low systems, *Atmos. Chem. Phys.*, 17, 3083-3095, 10.5194/acp-17-3083-2017, 2017.
- 637 Zhang, R., Wang, Y., Smeltzer, C., Qu, H., Koshak, W., and Boersma, K. F.: Comparing OMI-
638 based and EPA AQS in situ NO₂ trends: towards understanding surface NO_x emission changes,
639 *Atmos. Meas. Tech.*, 11, 3955-3967, 10.5194/amt-11-3955-2018, 2018.
- 640 Zhang, Y., and Wang, Y.: Climate-driven ground-level ozone extreme in the fall over the
641 Southeast United States, *Proc. Natl. Acad. Sci. U.S.A.*, 113, 10025-10030,
642 10.1073/pnas.1602563113, 2016.
- 643 Zhao, C., and Wang, Y.: Assimilated inversion of NO_x emissions over east Asia using OMI NO₂
644 column measurements, *Geophys. Res. Lett.*, 36, 10.1029/2008GL037123, 2009.
- 645 Zhao, C., Wang, Y., Choi, Y., and Zeng, T.: Summertime impact of convective transport and
646 lightning NO_x production over North America: modeling dependence on meteorological
647 simulations, *Atmos. Chem. Phys.*, 9, 4315-4327, 10.5194/acp-9-4315-2009, 2009a.
- 648 Zhao, C., Wang, Y., and Zeng, T.: East China plains: A “basin” of ozone pollution, *Environ. Sci.*
649 *Technol.*, 43, 1911-1915, 10.1021/es8027764, 2009b.
- 650 Zhao, C., Wang, Y., Yang, Q., Fu, R., Cunnold, D., and Choi, Y.: Impact of East Asian summer
651 monsoon on the air quality over China: View from space, *J. Geophys. Res.-Atmos.*, 115,
652 10.1029/2009JD012745, 2010.

653

Table 1. Summary of trends of satellite NO₂ TVCD products, NO₂ surface measurements, and EPA anthropogenic NO_x emissions during from different studies

Studies	Datasets	Period 1 ¹		Period 2		Period 3		Slowdown ratio ³
		Time	Trend (yr ⁻¹) ²	Time	Trend (yr ⁻¹)	Time	Trend (yr ⁻¹)	
This study for CONUS “urban” sites ⁴	GOME-2B ⁵ (36 × 36 km ²)					2013 - 2017	-8.2 ± 3.0%	
	SCIAMACHY (36 × 36 km ²)	2003 – 2011	-6.3 ± 1.1%					
	OMI-NASA (36 × 36 km ²)	2005 – 2011	-8.6 ± 1.2%			2011 – 2016	-6.1 ± 3.6%	-29% ²
	OMI-BEHR (36 × 36 km ²)	2005 – 2011	-8.2 ± 1.3%			2011 – 2016	-4.4 ± 1.6%	-46%
	OMI-QA4ECV (36 × 36 km ²)	2005 – 2011	-7.7 ± 1.4%			2011 - 2017	-4.2 ± 0.5%	-46%
	Updated EPA NO _x emissions ⁶	2003 – 2011	-6.5 ± 0.8%			2011 - 2017	-5.1 ± 0.3%	-22%
This study for AQS “urban” sites	GOME-2B (36 × 36 km ²)					2013 - 2017	-10.2 ± 2.9%	
	SCIAMACHY (36 × 36 km ²)	2003 - 2011	-7.6 ± 1.1%					
	OMI-NASA (36 × 36 km ²)	2005 - 2011	-9.0 ± 0.8%			2011 – 2016	-7.2 ± 3.8%	-20%
	OMI-BEHR (36 × 36 km ²)	2005 - 2011	-8.9 ± 0.3%			2011 – 2016	-6.2 ± 2.6%	-30%
	OMI-QA4ECV (36 × 36 km ²)	2005 - 2011	-9.0 ± 0.8%			2011 - 2017	-5.4 ± 0.9%	-40%
	NO ₂ surface VMR ⁷	2003 - 2011	-6.5 ± 1.2%			2011 - 2017	-5.9 ± 0.8%	-9%
(Russell et al., 2012) ⁸	BEHR v2.1 NO ₂ TVCD (0.05°×0.05°)	2005 - 2007	-6 ± 5% (-6.2%) ⁹	2007 - 2009	-8 ± 5% (-8.4%)	2009 - 2011	-3 ± 4% (-3.0%)	-52%
	Updated EPA NO _x emissions		-6.0%		-10.0%		-2.4%	-60%
(Tong et al., 2015) ¹⁰	NASA v2.1 NO ₂ TVCD (pixels < 50 × 24 km ²)	2005 - 2007	-7.3% (-7.6%)	2008 - 2009	-9.2% (-11.4%)	2010 - 2012	-2.8% (-4.4%)	-42%
	BEHR v2.1 NO ₂ TVCD (pixels < 50 × 24 km ²)		-8.9% (-9.3%)		-9.1% (-11.8%)		-3.6% (-6.0%)	-35%
	NO ₂ surface VMR		-6.0% (-6.2%)		-10.8% (-13.2%)		-3.4% (-5.4%)	-13%
	Updated EPA NO _x emissions		-6.0%		-10.0%		-3.4%	-43%
(Lamsal et al., 2015) ¹¹	NASA v2.1 NO ₂ TVCD (0.1°×0.1°)	2005 - 2008	-4.8 ± 1.9% (-5.1%)			2010 - 2013	-1.2 ± 1.2% (-1.2%)	-76%
	NO ₂ surface VMR		-3.7 ± 1.5% (-3.8%)				-2.1 ± 1.4% (-2.1%)	-45%
	Updated EPA NO _x emissions		-6.4%				-4.0%	-38%
(Jiang et al., 2018) ¹¹	NASA v3 NO ₂ TVCD (0.5°×0.667°)	2005 - 2009	-10.2 ± 1.8% (-9.8%)			2011-2015	-3.2 ± 1.6% (-3.2%)	-67%
	QA4ECV v2 NO ₂ TVCD (0.5°×0.667°)		-9.6 ± 1.7% (-9.3%)				-2.6 ± 1.8% (-2.6%)	-72%
	BEHR v2.1 NO ₂ TVCD (0.5°×0.667°)		-8.5 ± 1.8% (-8.2%)				-2.1 ± 1.6% (-2.1%)	-74%
	NO ₂ surface VMR		-6.6 ± 1.4% (-6.4%)				-2.6 ± 1.5% (-2.6%)	-59%
	Updated EPA NO _x emissions		-7.8%				-5.0%	-36%

655

¹ Since different studies used different time division methods, we list the period of each study in the table.

656

² Trends are based on an exponential model ($E(y) = E_0 \times r^{y-y_0}$: “y” denotes year and “y₀” denotes the initial year; “E(y)” denotes the value at year “y” and “E₀” denotes the value at the initial year; r-1 is the relative trend).

657

³ Slowdown ratios = Trend in “period 3” / Trend in “period 1” – 1.

658

⁴ Trends in our study are calculated based on the national seasonal trends shown in Table 3.

659

⁵ The information on satellite products used in this study is summarized in Table S2.

660

⁶ We updated EPA anthropogenic NO_x emissions with the newest Continuous Emission Monitoring Systems (CEMS) datasets. Figure S24 shows the comparison between our updated and original EPA anthropogenic NO_x emissions (EPA, 2018).

661

⁷ Denote the averaged trends of 13:00 and 10:00 LT based on the values in Table 3.

662 ⁸ The study used NO₂ TVCD from urban and power plant grid cells across the U.S.

663 ⁹ Since previous studies used linear models to calculate trends and the results are sensitive to their calculation methods and the selection of initial years, we recalculate the trends based on the above exponential model, which makes all the results

664 consistent. Our results are those bold numbers inside the parentheses, while the numbers in normal fonts are from the original publications.

665 ¹⁰ The study uses NO₂ TVCD and surface concentrations from Los Angeles, Dallas, Houston, Atlanta, Philadelphia, Washington, D.C., New York, and Boston.

666 ¹¹ The two studies used the EPA Air Quality System (AQS) NO₂ surface measurements and coincident satellite NO₂ TVCD data over the U.S.

667 **Table 2.** Properties of urban and rural regions in July 2011

type	Surface area fraction ¹	Anthropogenic NO _x emissions (× 10 ¹⁰ molecules cm ⁻² s ⁻¹)	β at 13:00 – 14:00 LT	γ at 13:00 – 14:00 LT	β at 10:00 – 11:00 LT	γ at 10:00 – 11:00 LT
Urban/CONUS ²	17.3%	29.9	2. 53 ± 1.00 .9	1. 54 ± 0. 43	2. 64 ± 1. 98	1. 65 ± 1. 20
Rural/CONUS	82.7%	2.7	16.98 .1 ± 16.48 .7	8.53 .1 ± 11.73 .9	12.25 .9 ± 14.08 .0	6.42 .8 ± 11.65 .8
Urban/AQS	87.7%	71.0	1. 65 ± 0. 87	1.2 ± 0.4	1.7 ± 1. 10	1.3 ± 0. 65
Rural/AQS	12.3%	5.7	8.75 .0 ± 9.92 .0	5.22 .5 ± 8.81 .3	5.44 .3 ± 15.13 .2	3.82 .7 ± 11.72 .6

668 ¹ “Fraction” denotes the percentages of “urban” or “rural” data points for the whole CONUS or all AQS sites.

669 ² “Urban-CONUS” denote CONUS “urban” grid cells; “Urban-AQS” denote AQS “urban” site grid cells.

670

671

672

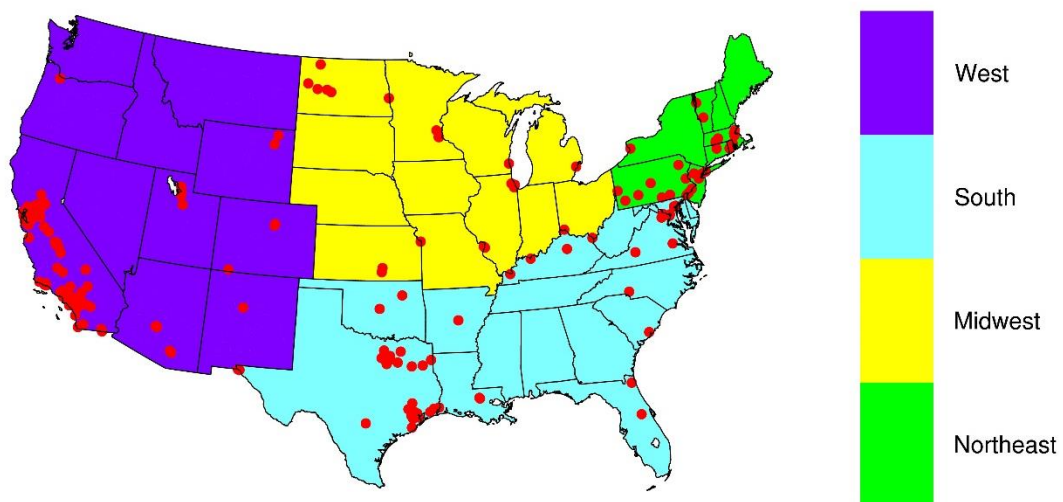
673

Table 3. Summary of national trends of updated EPA anthropogenic NO_x emissions, AQS NO₂ surface concentrations at 13:00 – 14:00 and 10:00 – 11:00 LT, and satellite NO₂ TVCD products for 4 seasons during different periods¹

		Spring		Summer		Autumn		Winter	
		AQS site	CONUS	AQS site	CONUS	AQS site	CONUS	AQS site	CONUS
AQS NO ₂ VMR at 13:00 -14:00	2003 – 2011	-7.3 ± 1.4%		-7.4 ± 0.9%		-6.7 ± 1.8%		-5.2 ± 0.8%	
	2011 – 2017	-5.3 ± 1.6%		-6.4 ± 1.2%		-7.3 ± 2.5%		-6.0 ± 2.8%	
AQS NO ₂ VMR at 10:00 – 11:00	2003 – 2011	-7.1 ± 1.6%		-7.6 ± 1.5%		-6.2 ± 2.2%		-4.4 ± 1.6%	
	2011 – 2017	-4.4 ± 1.4%		-6.1 ± 1.8%		-6.3 ± 2.5%		-5.2 ± 2.4%	
SCIAMACHY	2003 – 2011	-8.8 ± 3.4%	-6.9 ± 1.1%	-8.2 ± 1.6%	-5.2 ± 1.2%	-6.8 ± 2.4%	-5.6 ± 2.1%	-6.4 ± 7.4%	-7.5 ± 5.5%
	2011 – 2017								
GOME2B	2003 – 2011								
	2013 – 2017	-10.2 ± 7.8%	-8.3 ± 16.9%	-6.4 ± 14.0%	-5.3 ± 4.0%	-10.5 ± 41.6%	-6.9 ± 13.2%	-13.6 ± 15.1%	-12.3 ± 78.9%
OMI-QA4ECV	2005 – 2011	-9.3 ± 5.6%	-8.3 ± 4.6%	-8.3 ± 2.4%	-5.9 ± 5.2%	-10.0 ± 4.2%	-7.4 ± 2.4%	-8.3 ± 2.1%	-9.3 ± 5.2%
	2011 – 2017	-5.3 ± 6.0%	-4.3 ± 6.5%	-4.2 ± 3.0%	-4.9 ± 9.2%	-6.0 ± 1.8%	-3.8 ± 1.8%	-6.1 ± 25.6%	-3.8 ± 3.5%
OMI-NASA	2005 – 2011	-9.4 ± 5.0%	-9.6 ± 5.3%	-9.4 ± 2.8%	-7.1 ± 2.9%	-9.4 ± 3.2%	-8.1 ± 2.8%	-7.8 ± 3.6%	-9.5 ± 16.6%
	2011 – 2016	-4.4 ± 18.9%	-3.8 ± 7.5%	-5.7 ± 6.7%	-4.5 ± 5.3%	-6.0 ± 3.1%	-4.6 ± 3.9%	-12.8 ± 7.8%	-11.4 ± 6.6%
OMI-BEHR	2005 – 2011	-9.1 ± 5.3%	-8.9 ± 5.8%	-8.7 ± 2.4%	-6.4 ± 3.2%	-9.2 ± 3.2%	-8.0 ± 3.1%	-8.5 ± 10.6%	-9.4 ± 23.0%
	2011 – 2016	-3.8 ± 4.4%	-3.0 ± 4.0%	-5.4 ± 7.0%	-3.9 ± 6.6%	-5.6 ± 13.2%	-4.1 ± 14.0%	-9.9 ± 5.2%	-6.7 ± 5.9%
EPA	2003 – 2011					-6.5 ± 0.8%			
	2011 – 2017					-5.1 ± 0.3%			

674

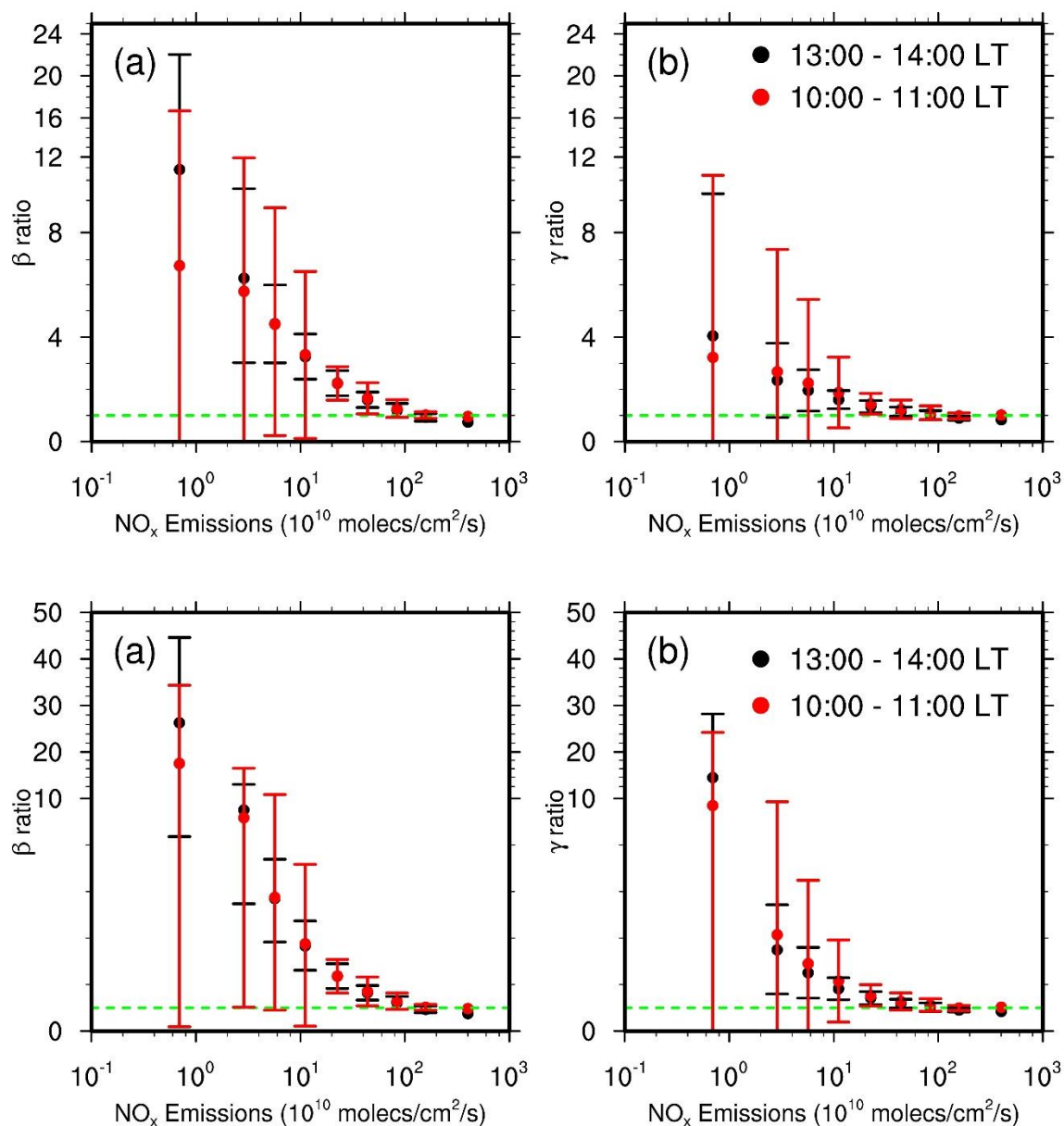
¹ We calculate trends by using the exponential model described in Table 1.



675
676 Figure 1. Region definitions and locations of NO₂ surface observation sites used in this study.

677

678



679

680

Figure 2. Distributions of β (panel a) and γ (panel b) ratios as a function of anthropogenic NO_x emissions on weekdays for July 2011 over the CONUS. “13:00 – 14:00 LT” is for OMI, and “10:00 – 11:00” LT is for SCIAMACHY and GOME-2A/2B. The data are binned into nine groups based on anthropogenic NO_x emissions: $E \in (0, 2^1), [2^1, 2^2), [2^2, 2^3), [2^3, 2^4), [2^4, 2^5), [2^5, 2^6), [2^6, 2^7), [2^7, 2^8), [2^8, 2^9) \times 10^{10} \text{ molecules cm}^{-2} \text{ s}^{-1}$. Here, $(0, 2^1)$ denotes $0 < \text{emissions} < 2^1$, and $[2^1, 2^2)$ denotes $2^1 \leq \text{emissions} < 2^2$, similar to other intervals. The green dashed line denotes a value of 1. Error bars denote standard deviations.

688

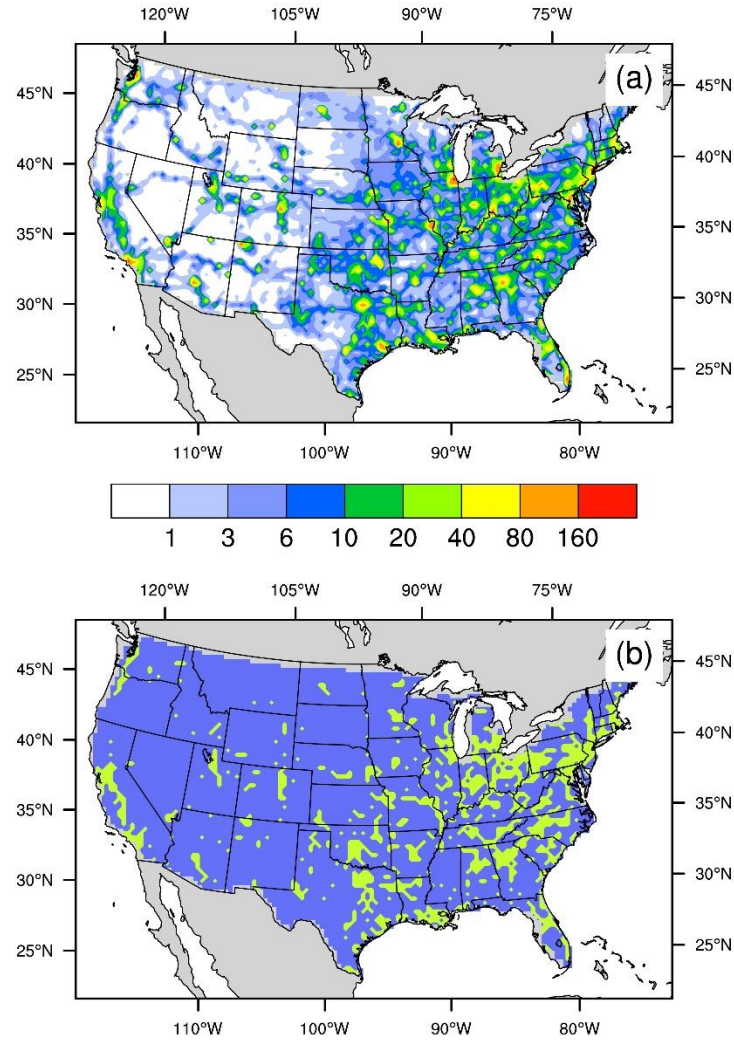


Figure 3. Spatial distributions of (a) anthropogenic NO_x emissions (unit: 10¹⁰ molecules cm⁻² s⁻¹) and (b) “urban” regions satisfying our selection criteria. In (b), light green and blue denote the resulting urban and rural regions, respectively.

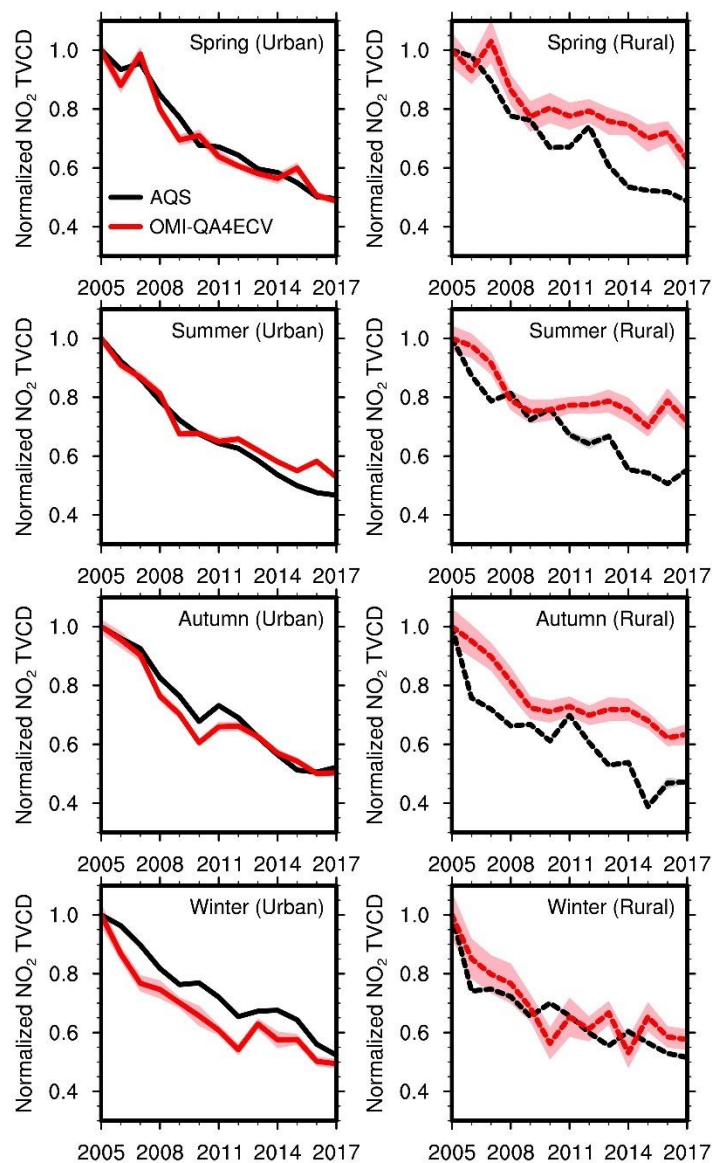


Figure 4. Relative annual variations of AQS NO_2 surface concentrations and coincident OMI-QA4ECV NO_2 TVCD in each season from 2005 – 2017 for urban (left panel) and rural (right panel) regions. The observation data are scaled by the corresponding 2005 values. Black and red lines denote AQS surface observations and OMI-QA4ECV NO_2 TVCDs, respectively. Shading in a lighter color is added to show the standard deviation of the results; when uncertainty is small due in part to a large number of data points, shading area may not show up.

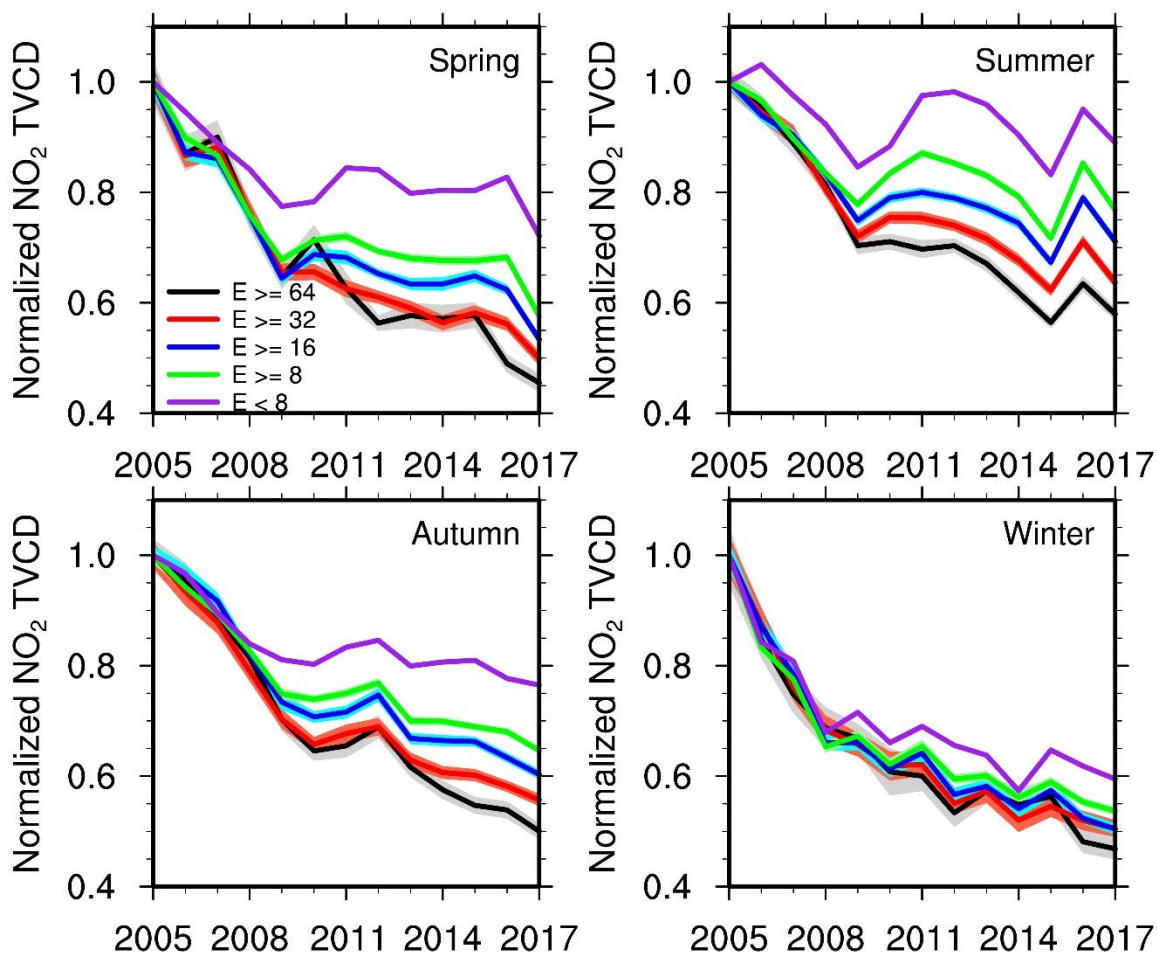


Figure 5. Relative annual variations of OMI-QA4ECV NO₂ TVCD for different anthropogenic NO_x-emission groups based on NEI2011 in each season from 2005 – 2017. “ $E \geq 64$ ” denotes grid cells with anthropogenic NO_x emissions over 64×10^{10} molecules cm⁻² s⁻¹. “ $E \geq 32$ ” denotes grid cells with anthropogenic NO_x emissions equal to or larger than 32×10^{10} molecules cm⁻² s⁻¹ but less than 64×10^{10} molecules cm⁻² s⁻¹. “ $E \geq 16$ ” and “ $E \geq 8$ ” have similar meanings as “ $E \geq 32$ ”. “ $E < 8$ ” denotes grid cells with anthropogenic NO_x emissions less than 8×10^{10} molecules cm⁻² s⁻¹. Shading in a lighter color is added to show the standard deviation of the results; when uncertainty is small due in part to a large number of data points, shading area may not show up.

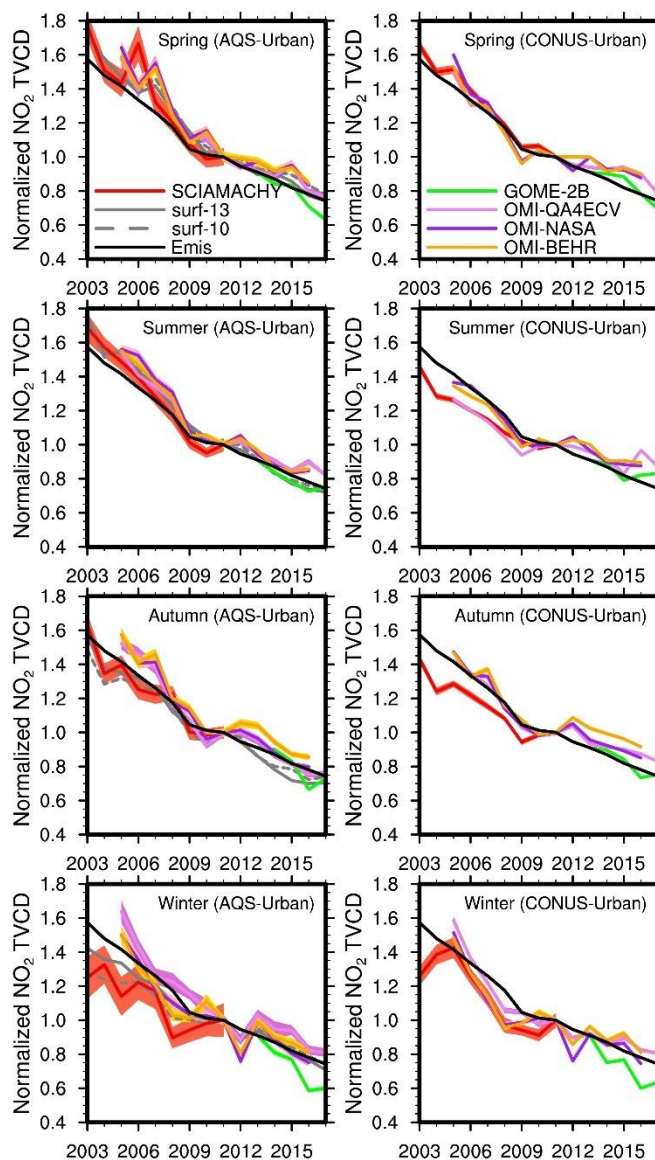
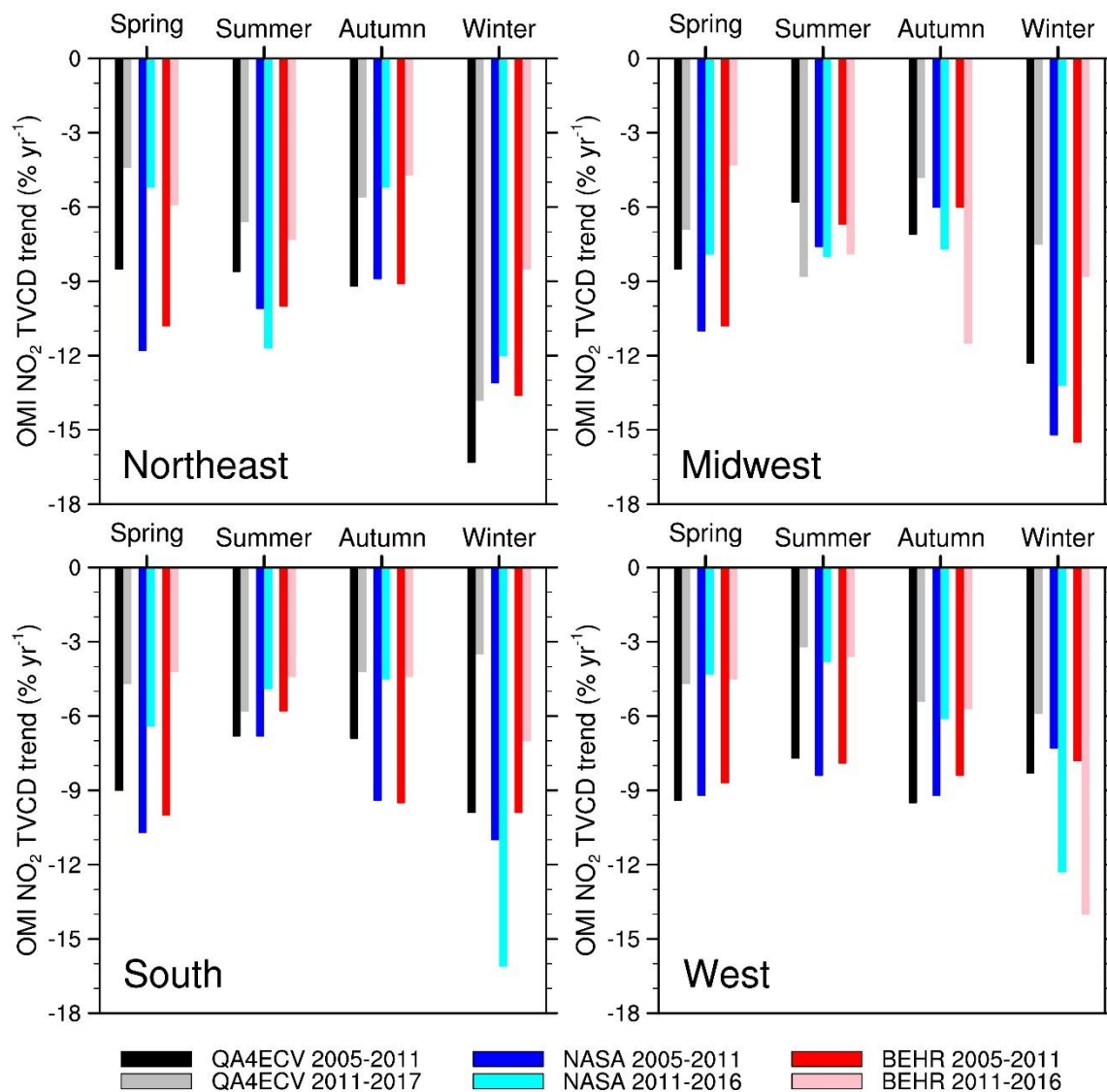


Figure 6. Relative variations of AQS NO_2 surface measurements at 13:00-14:00 and 10:00-11:00 LT, updated EPA anthropogenic NO_x emissions, and satellite NO_2 TVCD data over the AQS urban sites (left column) and the CONUS urban regions (right column) for 4 seasons. AQS NO_2 surface measurements are not included in the right column. All datasets are scaled by their corresponding values in 2011 except for GOME-2B. For GOME-2B, we firstly normalized the values in each season to the corresponding 2013 values and plotted the relative changes from the 2013 EPA point of each season to make the GOME-2B relative variations comparable to the other datasets. Shading in a lighter color is added to show the standard deviation of the results; when uncertainty is small due in part to a large number of data points, shading area may not show up.



728
 729 Figure 7. Pre- and post-2011 OMI NO₂ TVCD trends for 4 seasons in the urban regions of
 730 Northeast, Midwest, South, and West. Black bars denote OMI-QA4ECV NO₂ TVCD trends from
 731 2005 – 2011; gray bars denote the corresponding trends during 2011 – 2017. Blue bars denote
 732 OMI-NASA trends from 2005 – 2011; cyan bars denote NASA-OMI trends from 2011 – 2016.
 733 Red bars denote BEHR-OMI trends from 2005 – 2011; pink bars denote OMI-BEHR trends from
 734 2011 – 2016.

735

Inferring the anthropogenic NO_x emission trend over the United States during 2003 - 2017 from satellite observations: Was there a flattening of the emission trend after the Great Recession?

Jianfeng Li¹, Yuhang Wang^{1*}

¹School of Earth and Atmospheric Sciences, Georgia Institute of Technology, Atlanta, Georgia, USA

* *Correspondence to* Yuhang Wang (yuhang.wang@eas.gatech.edu)

Figure Captions

Figure S1. Annual variation of NO_3^- wet deposition fluxes for each season from 2003 – 2017. The fluxes were scaled by the corresponding values in 2003. Shaded regions denote standard deviations. Monthly NO_3^- wet deposition observations are obtained from <https://nadp.slh.wisc.edu/data/NTN/ntnAllsites.aspx> (last access, September 29, 2019).

Figure S2. Comparison between original EPA anthropogenic NO_x emissions and updated EPA anthropogenic NO_x emissions with the newest Continuous Emission Monitoring Systems (CEMS) measurements.

Figure S3. Daily OMI NO_2 TVCDs for July 2011 (a) and 2012 (b) in Atlanta (33.755°N , 84.39°W). Black circles are weekday values, and red circles are weekend values. We find significant daily variations of NO_2 TVCD from (a) and (b). The number of available measurements in July 2011 is much less than July 2012. We find clear larger NO_2 TVCD values on weekdays than on weekends in July 2011, but the difference between weekday and weekend TVCDs in July 2012 are not so obvious.

Figure S4. Hourly averaged ratios of FEM (a) and CAPS (b) to FRM NO_2 measurements in each season, respectively. The FEM/FRM ratios are computed from coincident FRM and FEM measurements from 2013 – 2015 at 4 sites. The CAPS/FRM ratios are calculated based on coincident CAPS and FRM data from 2015 – 2016 at 3 sites.

Figure S5. Annual variations of AQS NO_2 surface concentrations at different hours on weekdays in spring (a, b), summer (c, d), autumn (e, f), and winter (g, h). Left panels show absolute NO_2 concentrations, and right panels are their relative variations normalized to 2011. To conduct reliable and consistent comparisons, we only used monitoring sites satisfying the seasonal $RCI < 50\%$ and continuity criteria on weekdays from 2003 – 2017.

Figure S6. Distributions of (a) NO₂ TVCD fraction that is in the boundary layer (< 2810 m) at 13:00 – 14:00, (b) NO₂ TVCD fraction in the boundary layer (< 1290 m) at 10:00 – 11:00, (c) the fraction of soil NO_x emissions in all surface sources (anthropogenic + soil) on weekdays for July 2011. As the lifetime of NO₂ in the free troposphere (several days ~ 2 weeks) is much longer than that in the boundary layer (~ 10 hours), local lightning NO_x emissions cannot represent NO₂ VCDs in the free troposphere. In this study, we apply NO₂ VCD in the free troposphere to analyze the impact of lightning NO_x on the nonlinear relationships between anthropogenic NO_x emissions and NO₂ TVCDs and use lightning NO_x and NO₂ VCD in the free troposphere interchangeably in the following.

Figure S7. (a) Distributions of the fractions of surface NO_x emissions emitted by soil (“SoilNO_x”), the portions of NO₂ TVCDs in the boundary layer (“PBLVCD”), and the fractions of NO₂ TVCDs from anthropogenic NO_x emissions (“AnthroVCD”) as functions of NEI2011 anthropogenic NO_x emissions at 13:00 – 14:00 LT on weekdays for July 2011 over the CONUS.

The fraction of NO₂ TVCDs from anthropogenic NO_x emissions is equal to $\left(1 - \frac{E_{soil}}{E_{soil} + E_{anthropogenic}}\right) \times \left(\frac{TVCD_{boundary}}{TVCD_{boundary} + TVCD_{free}}\right)$, where E_{soil} denotes soil NO_x emissions,

$E_{anthropogenic}$ denotes anthropogenic NO_x emissions, $TVCD_{boundary}$ denotes NO₂ TVCDs in the boundary layer, and $TVCD_{free}$ denotes NO₂ TVCDs in the free troposphere. The calculated data are grouped into 9 bins as in Figure 2. (b) Same as (a), but for 10:00 – 11:00 LT. (c) Distributions of β_{Emis} , γ_{Emis} , β , and γ as functions of anthropogenic NO_x emissions at 13:00 – 14:00 LT on weekdays for July 2011 over the CONUS. β and γ are the same as Figure 2. β_{Emis} and γ_{Emis} denote β and γ values when no other factors are taken into consideration except for soil NO_x emissions, anthropogenic NO_x emissions, and NO₂ in the free troposphere. $\beta_{Emis} =$

$$\frac{15\% \times \left(\frac{E_{anthropogenic}}{E_{anthropogenic} + E_{soil}}\right) \left(\frac{TVCD_{boundary}}{TVCD_{boundary} + TVCD_{free}}\right)}{15\% \times \left(\frac{E_{anthropogenic}}{E_{anthropogenic} + E_{soil}}\right) \left(\frac{TVCD_{boundary}}{TVCD_{boundary} + TVCD_{free}}\right)} = \left(\frac{E_{anthropogenic} + E_{soil}}{E_{anthropogenic}}\right) \left(\frac{TVCD_{boundary} + TVCD_{free}}{TVCD_{boundary}}\right)^2$$

and $\gamma_{Emis} = \frac{15\%}{15\% \times \left(\frac{E_{anthropogenic}}{E_{anthropogenic} + E_{soil}} \right)} = \left(\frac{E_{anthropogenic} + E_{soil}}{E_{anthropogenic}} \right)$. It is noteworthy that here we assume no interactions between the boundary layer and the free troposphere, boundary NO_x are only related to soil and anthropogenic NO_x emissions, and lightning NO_x only affect NO_2 in the free troposphere. The assumptions are reasonable as the time scale (~ 1 week) of the interactions between the boundary layer and the free troposphere are much longer than NO_x lifetime in the boundary layer, and in this study, only a small fraction of lightning NO_x is distributed into the boundary layer. Therefore, β_{Emis} and γ_{Emis} roughly represent the contributions of background sources (lightning NO_x and soil NO_x) to β and γ values. The differences between β (γ) and β_{Emis} (γ_{Emis}) indicate the contribution of non-emission factors to β (γ) values, such as chemistry, transport, and dry and wet depositions. (d) Same as (c), but for 10:00 – 11:00 LT. From this figure, we find that both background sources (lightning NO_x + soil NO_x) and non-emission factors are important when considering the nonlinear relationships among NO_x emissions, NO_2 surface concentrations, and NO_2 TVCDs in low-anthropogenic- NO_x emission regions.

Figure S87. Same as Figure 4, but for AQS NO_2 surface concentrations and coincident GOME-2A NO_2 TVCD data during 2008 – 2016.

Figure S98. Relative variations of OMI-QA4ECV NO_2 TVCD data for urban regions (black lines) and the whole CONUS (red lines) from 2005 – 2017 in 4 seasons.

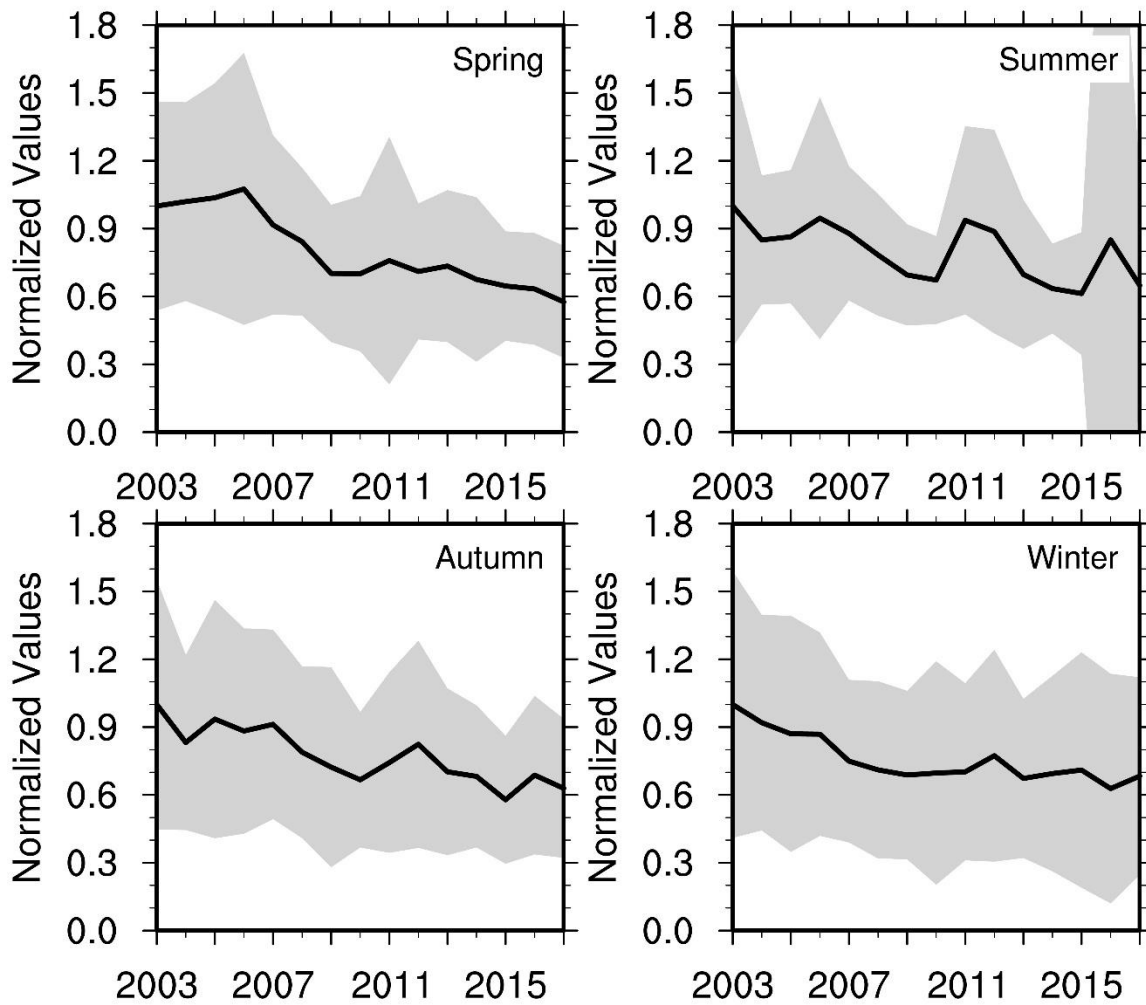
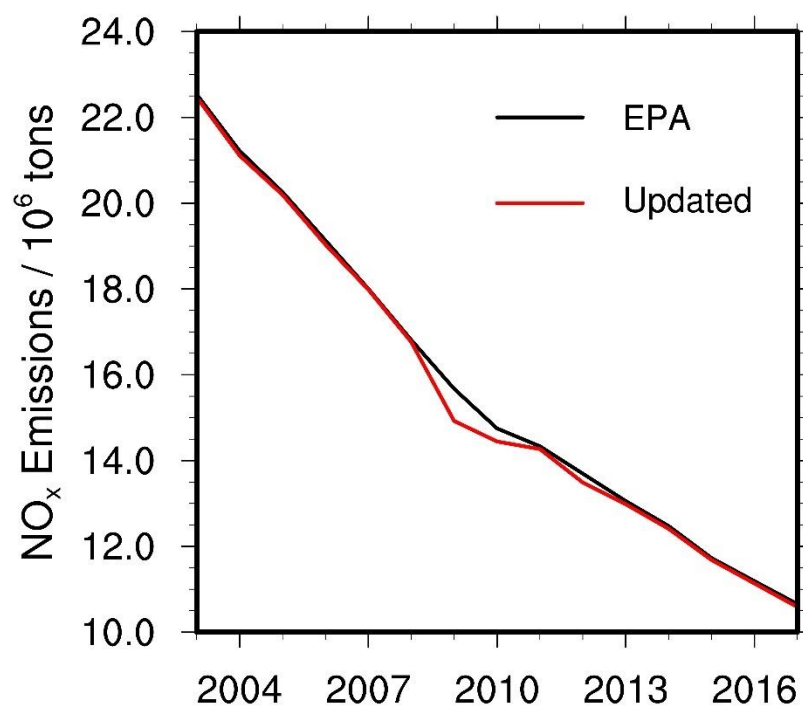


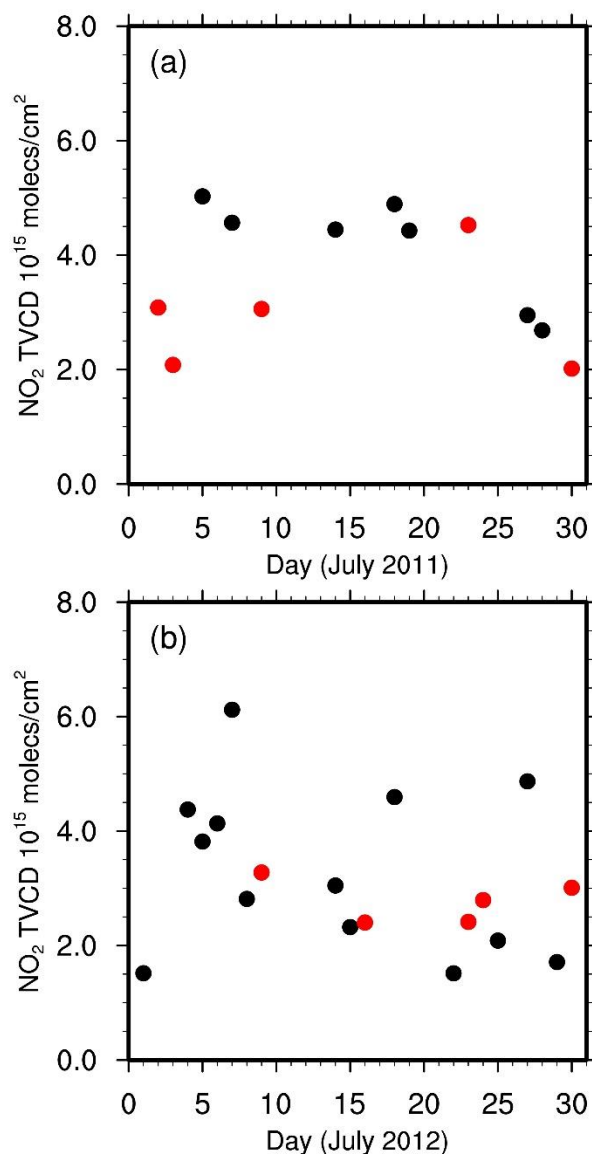
Figure S1. Annual variation of NO_3^- wet deposition fluxes for each season from 2003 – 2017. The fluxes were scaled by the corresponding values in 2003. Shaded regions denote standard deviations. Monthly NO_3^- wet deposition observations are obtained from <https://nadp.slh.wisc.edu/data/NTN/ntnAllsites.aspx> (last access, September 29, 2019).



80

81 Figure S24. Comparison between original EPA anthropogenic NO_x emissions and updated EPA
 82 anthropogenic NO_x emissions with the newest Continuous Emission Monitoring Systems
 83 (CEMS) measurements.

84



85

86 Figure S32. Daily OMI NO₂ TVCDs for July 2011 (a) and 2012 (b) in Atlanta (33.755° N, 84.39°
 87 W). Black circles are weekday values, and red circles are weekend values. We find significant
 88 daily variations of NO₂ TVCD from (a) and (b). The number of available measurements in July
 89 2011 is much less than July 2012. We find clear larger NO₂ TVCD values on weekdays than on
 90 weekends in July 2011, but the difference between weekday and weekend TVCDs in July 2012
 91 are not so obvious.

92

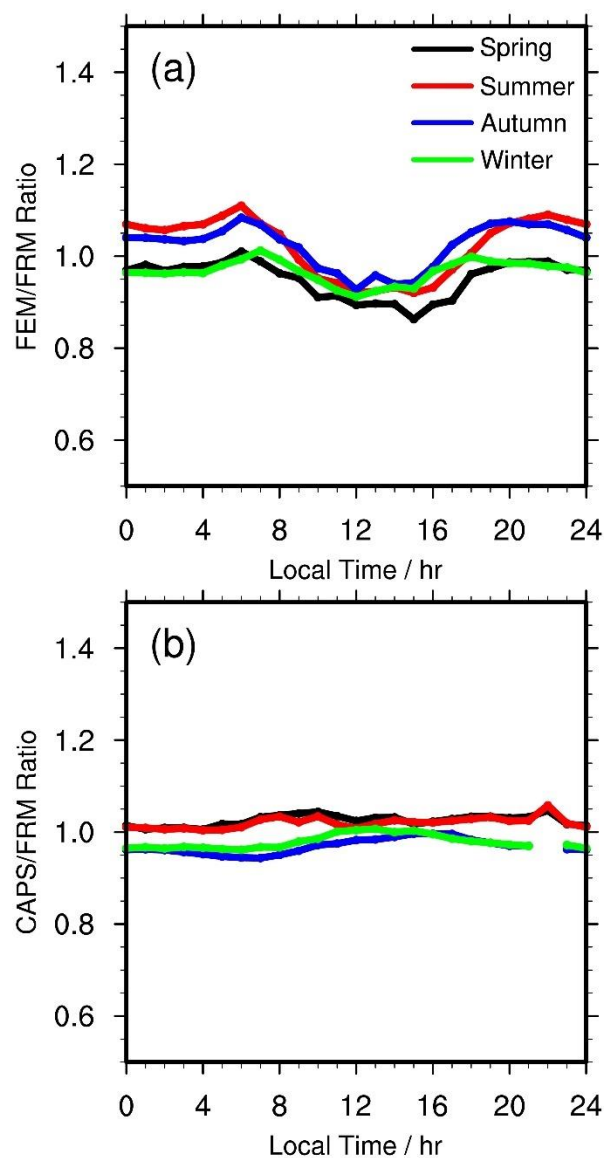
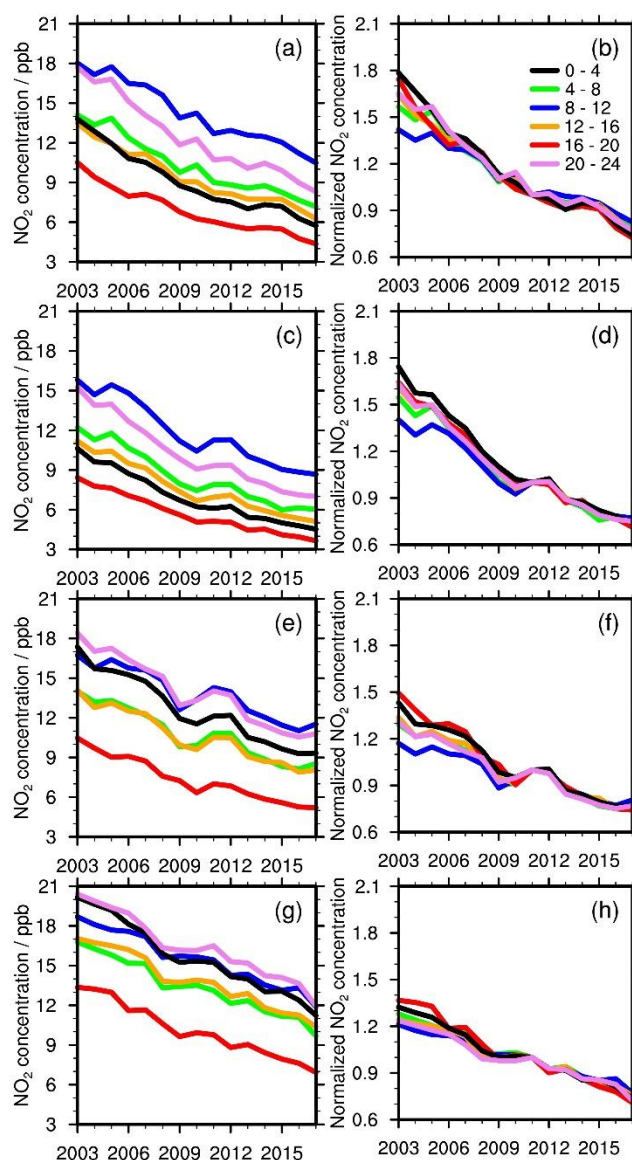


Figure S43. Hourly averaged ratios of FEM (a) and CAPS (b) to FRM NO₂ measurements in each season, respectively. The FEM/FRM ratios are computed from coincident FRM and FEM measurements from 2013 – 2015 at 4 sites. The CAPS/FRM ratios are calculated based on coincident CAPS and FRM data from 2015 – 2016 at 3 sites.



99

100 Figure S54. Annual variations of AQS NO₂ surface concentrations at different hours on weekdays
 101 in spring (a, b), summer (c, d), autumn (e, f), and winter (g, h). Left panels show absolute NO₂
 102 concentrations, and right panels are their relative variations normalized to 2011. To conduct
 103 reliable and consistent comparisons, we only used monitoring sites satisfying the seasonal *RCI* <
 104 50% and continuity criteria on weekdays from 2003 – 2017.

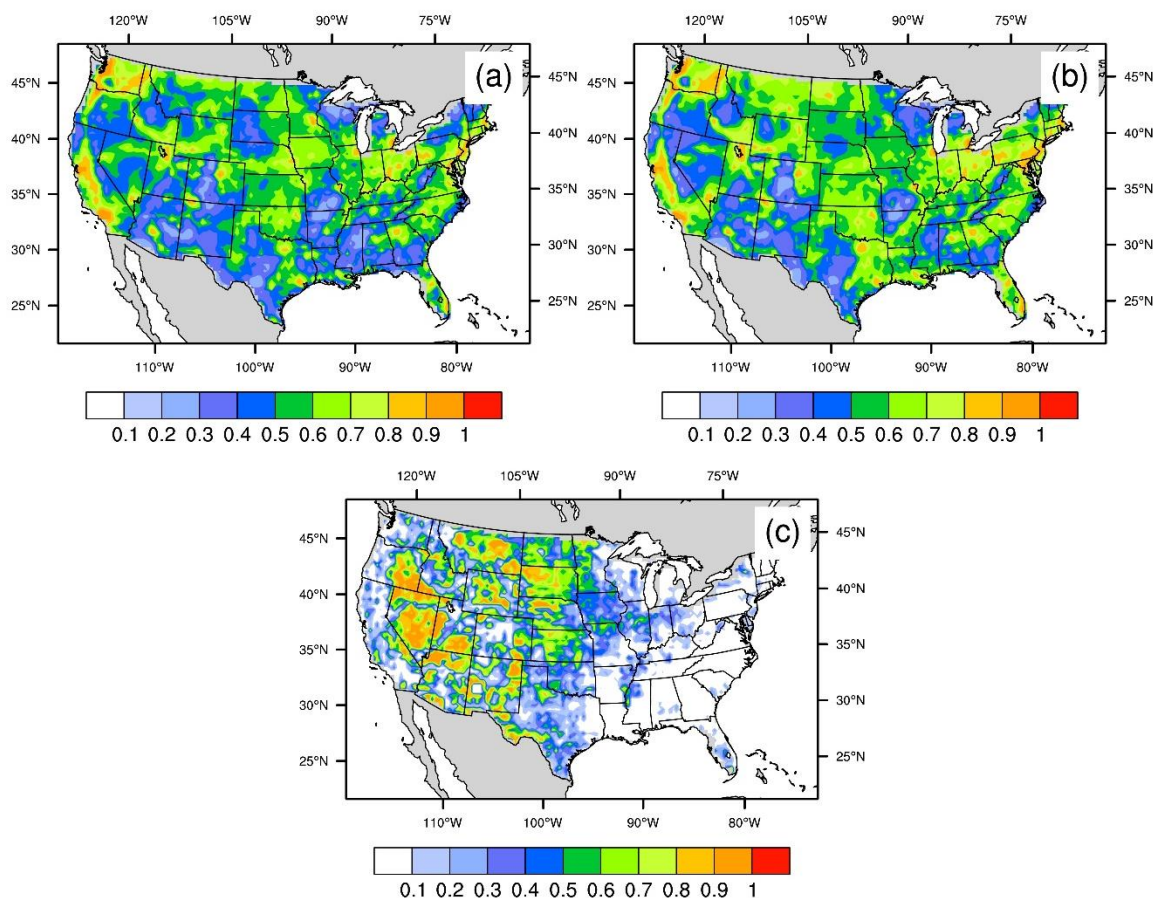


Figure S6. Distributions of (a) NO_2 TVCD fraction that is in the boundary layer (< 2810 m) at 13:00 – 14:00, (b) NO_2 TVCD fraction in the boundary layer (< 1290 m) at 10:00 – 11:00, (c) the fraction of soil NO_x emissions in all surface sources (anthropogenic + soil) on weekdays for July 2011. As the lifetime of NO_2 in the free troposphere (several days ~ 2 weeks) is much longer than that in the boundary layer (~ 10 hours), local lightning NO_x emissions cannot represent NO_2 VCDs in the free troposphere. In this study, we apply NO_2 VCD in the free troposphere to analyze the impact of lightning NO_x on the nonlinear relationships between anthropogenic NO_x emissions and NO_2 TVCDs and use lightning NO_x and NO_2 VCD in the free troposphere interchangeably in the following.

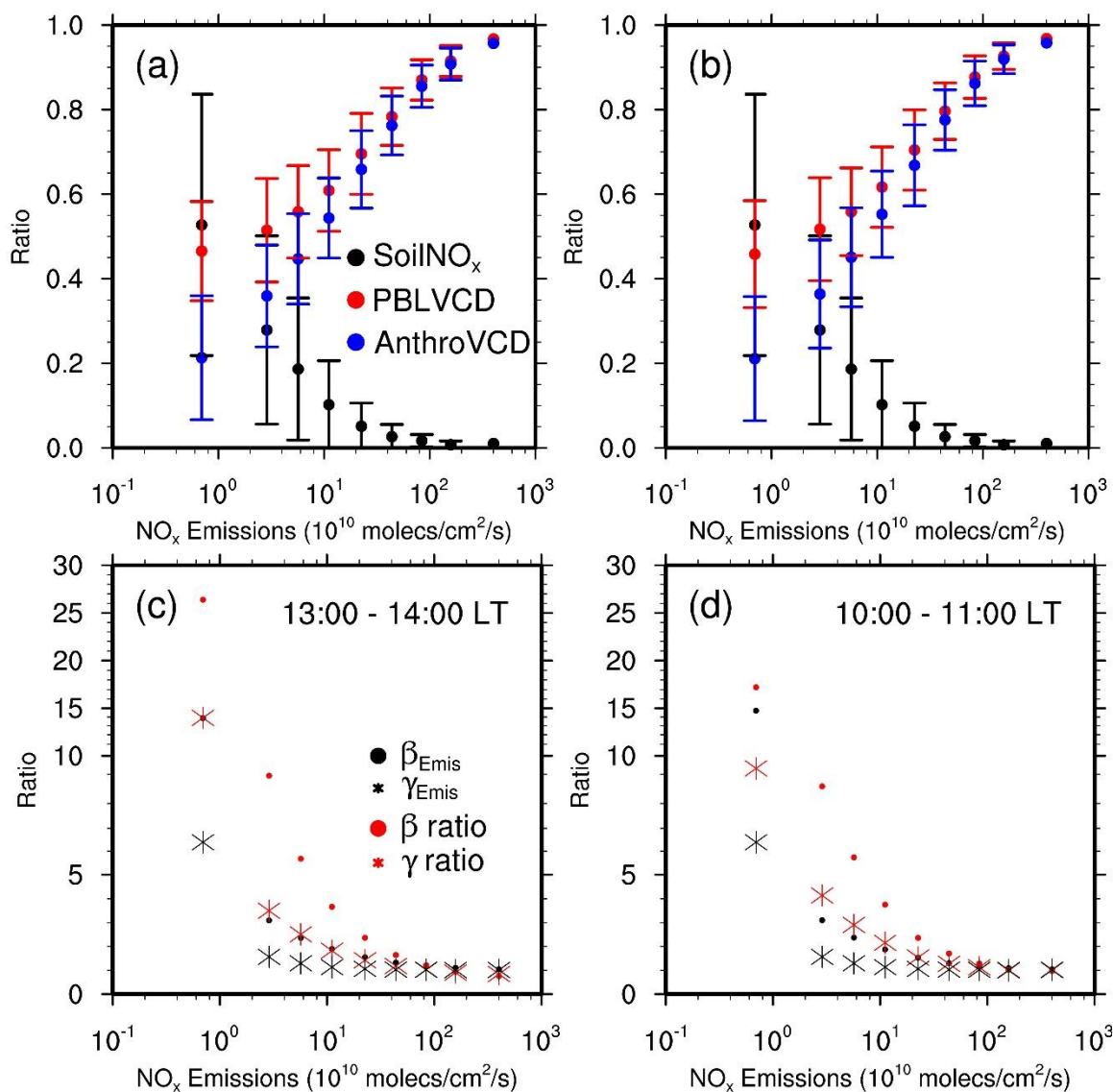


Figure S7. (a) Distributions of the fractions of surface NO_x emissions emitted by soil (“SoilNO_x”), the portions of NO_2 TVCDs in the boundary layer (“PBLVCD”), and the fractions of NO_2 TVCDs from anthropogenic NO_x emissions (“AnthroVCD”) as functions of NEI2011 anthropogenic NO_x emissions at 13:00 – 14:00 LT on weekdays for July 2011 over the CONUS. The fraction of NO_2 TVCDs from anthropogenic NO_x emissions is equal to $\left(1 - \frac{E_{\text{soil}}}{E_{\text{soil}} + E_{\text{anthropogenic}}}\right) \times \left(\frac{\text{TVCD}_{\text{boundary}}}{\text{TVCD}_{\text{boundary}} + \text{TVCD}_{\text{free}}}\right)$, where E_{soil} denotes soil NO_x emissions.

$E_{anthropogenic}$ denotes anthropogenic NO_x emissions, $TVCD_{boundary}$ denotes NO_2 TVCDs in the boundary layer, and $TVCD_{free}$ denotes NO_2 TVCDs in the free troposphere. The calculated data are grouped into 9 bins as in Figure 2. (b) Same as (a), but for 10:00 – 11:00 LT. (c) Distributions of β_{Emis} , γ_{Emis} , β , and γ as functions of anthropogenic NO_x emissions at 13:00 – 14:00 LT on weekdays for July 2011 over the CONUS. β and γ are the same as Figure 2. β_{Emis} and γ_{Emis} denote β and γ values when no other factors are taken into consideration except for soil NO_x emissions, anthropogenic NO_x emissions, and NO_2 in the free troposphere. $\beta_{Emis} =$

$$\frac{15\%}{15\% \times \left(\frac{E_{anthropogenic}}{E_{anthropogenic} + E_{soil}} \right) \left(\frac{TVCD_{boundary}}{TVCD_{boundary} + TVCD_{free}} \right)} = \left(\frac{E_{anthropogenic} + E_{soil}}{E_{anthropogenic}} \right) \left(\frac{TVCD_{boundary} + TVCD_{free}}{TVCD_{boundary}} \right)^2$$

and $\gamma_{Emis} = \frac{15\%}{15\% \times \left(\frac{E_{anthropogenic}}{E_{anthropogenic} + E_{soil}} \right)} = \left(\frac{E_{anthropogenic} + E_{soil}}{E_{anthropogenic}} \right)$. It is noteworthy that here we assume no interactions between the boundary layer and the free troposphere, boundary NO_x are only related to soil and anthropogenic NO_x emissions, and lightning NO_x only affect NO_2 in the free troposphere. The assumptions are reasonable as the time scale (~ 1 week) of the interactions between the boundary layer and the free troposphere are much longer than NO_x lifetime in the boundary layer, and in this study, only a small fraction of lightning NO_x is distributed into the boundary layer. Therefore, β_{Emis} and γ_{Emis} roughly represent the contributions of background sources (lightning NO_x and soil NO_x) to β and γ values. The differences between β (γ) and β_{Emis} (γ_{Emis}) indicate the contribution of non-emission factors to β (γ) values, such as chemistry, transport, and dry and wet depositions. (d) Same as (c), but for 10:00 – 11:00 LT. From this figure, we find that both background sources (lightning NO_x + soil NO_x) and non-emission factors are important when considering the nonlinear relationships among NO_x emissions, NO_2 surface concentrations, and NO_2 TVCDs in low-anthropogenic- NO_x emission regions.

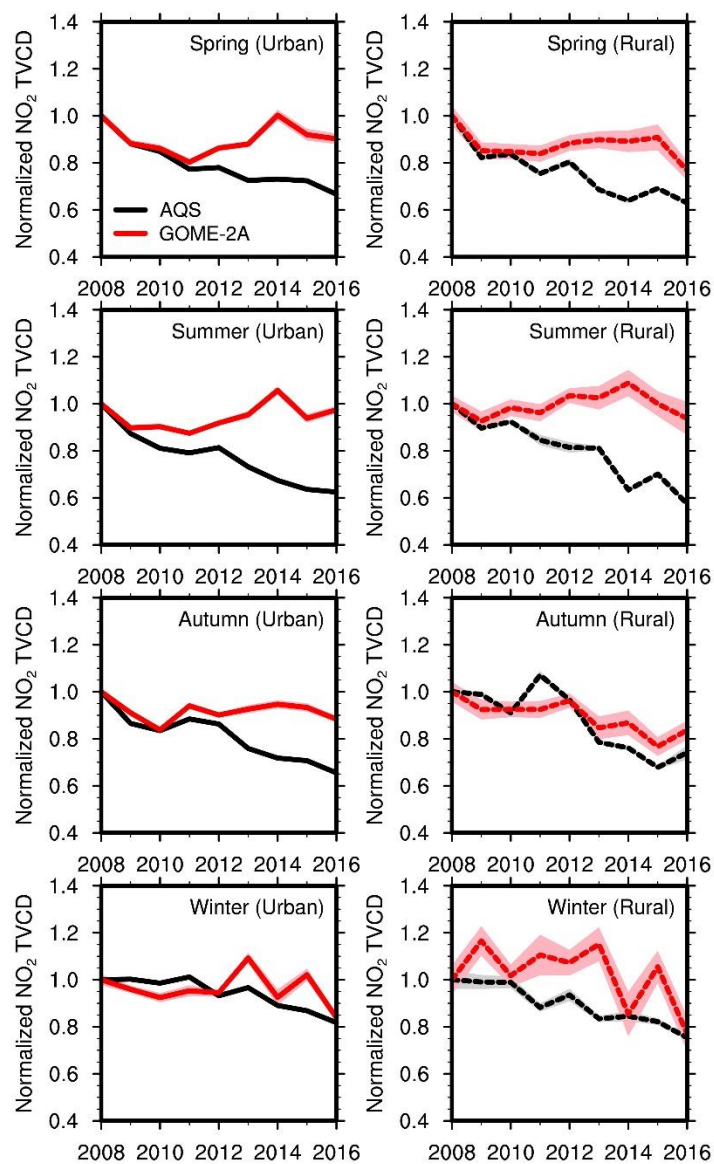
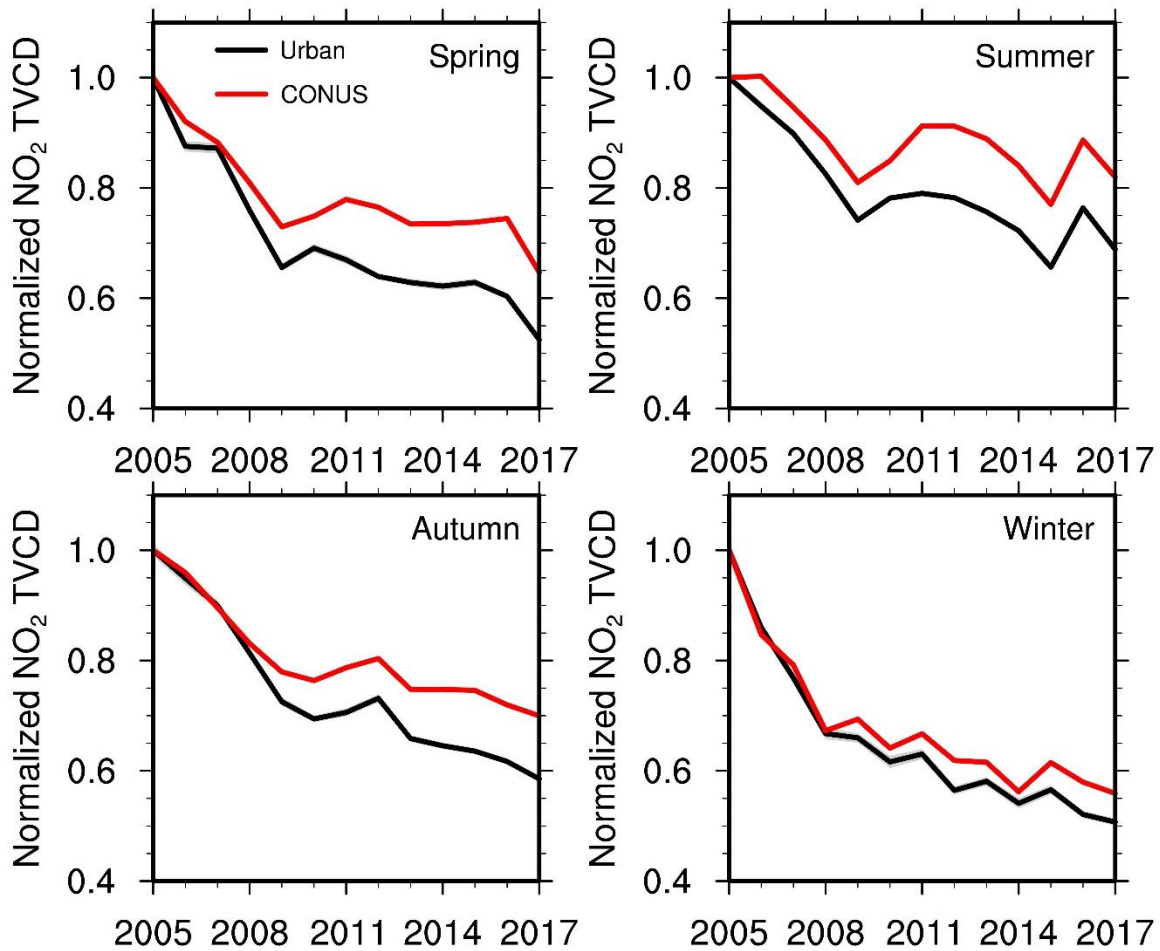


Figure S85. Same as Figure 4, but for AQS NO₂ surface concentrations and coincident GOME-2A NO₂ TVCD data during 2008 – 2016.



149

150 Figure S96. Relative variations of OMI-QA4ECV NO₂ TVCD data for urban regions (black lines)
 151 and the whole CONUS (red lines) from 2005 – 2017 in 4 seasons.

152

Inferring the anthropogenic NO_x emission trend over the United States during 2003 - 2017 from satellite observations: Was there a flattening of the emission trend after the Great Recession?

Jianfeng Li¹, Yuhang Wang^{1*}

¹School of Earth and Atmospheric Sciences, Georgia Institute of Technology, Atlanta, Georgia, USA

* *Correspondence to* Yuhang Wang (yuhang.wang@eas.gatech.edu)

12 **Table Captions**

13 Table S1. Summary of major satellite instruments for remote sensing of atmospheric NO₂ VCD in
14 the past decade

15 Table S2. Summary of satellite NO₂ TVCD products and their retrieval information

16 Table S3. Selection criteria for satellite NO₂ TVCD pixel data

17 Table S4. Summary of annual trends of AQS NO₂ surface concentrations and satellite NO₂ TVCD
18 products in each region during different periods

19 **Table S1. Summary of major satellite instruments for remote sensing of atmospheric NO₂ VCD in the past decade**

Instrument	Satellite	Launch date	End date	Operator	Equator crossing time (local time)	UV/Vis Spectral range (nm)	Spectral resolution (nm)	Swath length (km)	Nadir pixel resolution (km × km)	Global coverage (days)
SCIAMACHY	ENVISAT ¹	03/01/2002 ²	04/08/2012 ²	ESA ³	10:00 ¹	240 – 805 ⁴	0.24 – 0.48 ⁴	960 ⁵	60 × 30 ⁵	6 ⁵
GOME-2A	MetOp-A ⁶	10/19/2006 ⁶	in operation	EUMETSAT ⁷	9:30 ⁸	240 – 790 ⁸	0.26 – 0.51 ⁸	1920 before Jul. 15 th , 2013; 960 after Jul. 15 th , 2013 ⁸	80 × 40 before Jul. 15 th , 2013; 40 × 40 after Jul. 15 th , 2013 ⁸	1.5 ⁹
GOME-2B	MetOp-B ⁶	09/17/2012 ⁶	In operation	EUMETSAT	9:30 ⁸	240 – 790 ⁸	0.26 – 0.51 ⁸	1920 ⁸	80 × 40 ⁸	1.5 ⁹
OMI	EOS-Aura ¹⁰	07/152004 ¹⁰	In operation	NASA	13:45 ¹⁰	270 – 500 ¹¹	0.45 – 1.0 ¹¹	2600 ¹¹	24 × 13 ¹¹	1 ¹¹

20 ¹ Refer to <https://earth.esa.int/web/guest/missions/esa-operational-eo-missions/envisat>
21 ² Refer to <https://en.wikipedia.org/wiki/Envisat>
22 ³ The European Space Agency
23 ⁴ Refer to <http://www.iup.uni-bremen.de/sciamachy/instrument/performance/index.html>
24 ⁵ Refer to Boersma et al. (2008), Boersma et al. (2009), and (Lee et al., 2009)
25 ⁶ Refer to <https://www.eumetsat.int/website/home/Satellites/CurrentSatellites/Metop/index.html>
26 ⁷ The European Organization for the Exploitation of Meteorological Satellites
27 ⁸ Refer to EUMETSAT (2015)
28 ⁹ Refer to Lee et al. (2009) and Wang et al. (2017)
29 ¹⁰ Refer to <https://aura.gsfc.nasa.gov/>
30 ¹¹ Refer to <https://aura.gsfc.nasa.gov/omi.html>

31 **Table S2. Summary of satellite NO₂ TVCD products and their retrieval information**

NO ₂ TVCD products	Version	Available period	DOAS fitting method	Stratosphere–troposphere separation	Fitting window (nm)	Albedo / reflectance	A priori profiles	Radiative transfer model	Cloud	Uncertainty
GOME-2B	TM4NO2A (2.3)	12/20/2012 – current	Intensity fit ¹	Assimilation of satellite total slant columns in the TM4 model ^{2, 3}	405 – 465 ¹	Climatology albedo from 3 years of OMI data ⁴	TM4 (2° × 3°) ²	DAK ²	FRESCO+ (Oxygen A-band around 760 nm) ⁵	1.0 × 10 ¹⁵ molecules/cm ² + 25% ²
SCIAMACHY	QA4ECV (v1.1)	08/02/2002 – 04/08/2012	Optical Density ^{1, 6}	Assimilation of OMI total slant columns in the TM5 - MP model ^{6, 7}	425 – 465 ⁶	Climatology albedo based on SCIAMACHY ⁸	TM5-MP (1° × 1°) ⁶	DAK	FRESCO+	35% - 45% over polluted scenes; > 100% over background regions (Pacific Ocean) ⁶
GOME-2A	QA4ECV (v1.1)	02/01/2007 – 12/31/2016			405 – 465 ^{1, 6}	Climatology albedo based on GOME-2A ⁸			FRESCO+	
OMI-QA4ECV	QA4ECV (v1.1)	10/012004 – Current			405 – 465 ^{1, 6}	Climatology albedo from 5 years of OMI data ⁶			Improved O ₂ -O ₂ (477 nm) ⁹	
OMI-NASA	SPv3	01/01/2005 – 07/31/2017			402 – 465 ^{1, 10}	OMI climatology albedo ¹⁰	GMI (1° × 1.25°) ¹⁰	TMORAD ¹⁰	O ₂ -O ₂ (477 nm) ^{10, 11}	SPv2.1 TVCD has uncertainties of about 30% under clear-sky conditions to about 60% under cloudy conditions ¹² , and the relative difference between SPv3 and SPv2.1 is less than ~20% ¹⁰ .
OMI-BEHR ¹³	v3.0B	01/01/2005 – 07/31/2017	Stepwise intensity fit with monthly averaged solar irradiance spectrum ^{1, 10}	Based on OMI total slant columns over regions with low estimated TVCD contributions (TVCD contributions less than 0.3 × 10 ¹⁵ molecules/cm ²) ¹⁰		Based on MCD43D BRDF product (for land) and model parameterization (for ocean)	WRF-Chem (12 km)			

32 ¹ Refer to Zara et al. (2018)

33 ² Refer to Boersma et al. (2011). “TM4” is the Tracer Model, version 4. “DAK” is the Doubling-Adding KNMI (DAK) radiative transfer model.

34 ³ Refer to Williams et al. (2009)

35 ⁴ Refer to Kleipool et al. (2008)

36 ⁵ Refer to Wang et al. (2017) and Wang et al. (2008)

37 ⁶ Refer to Boersma et al. (2018)

38 ⁷ Refer to Williams et al. (2017)

39 ⁸ Refer to Tilstra et al. (2017)

40 ⁹ Refer to Veeffkind et al. (2016)

41 ¹⁰ Refer to Bucsela et al. (2013), Bucsela et al. (2016), Krotkov et al. (2017), and Marchenko et al. (2015). “TMORAD” is the TMOS radiative transfer model.

42 ¹¹ Refer to Acarreta et al. (2004)

43 ¹² Refer to Lamsal et al. (2014), Oetjen et al. (2013), and Tong et al. (2015)

44 ¹³ Refer to Laughner et al. (2018). OMI-BEHR uses the SCD from OMI-NASA SPv3 but updates inputs for the AMF calculation, such as a prior NO₂ vertical profiles and surface reflectance. Besides, OMI-BEHR only provides NO₂ TVCD over the contiguous

45 United States (CONUS). As in this study, we used the OMI-NASA datasets archived in the OMI-BEHR product, so we only obtained OMI-NASA datasets extended to July 31, 2017.

46 ¹⁴ Average uncertainty over the CONUS is calculated based on the file from <http://behr.cchem.berkeley.edu/behr/BEHR-us-uncertainty.hdf>

47 **Table S3. Selection criteria for satellite NO₂ TVCD pixel data**

NO ₂ TVCD products	Period	Solar zenith angle	albedo	Cloud radiance fraction	Snow or ice covered	AMFtrop/AMFgeo	Flag for retrieval success	Retrieval quality flag	Rows in swath
GOME-2B	01/01/2013 – 12/31/2017	< 80°	<= 0.3	<= 50%	No	> 0.2	Yes		All
SCIAMACHY	01/01/2003 – 12/31/2011	< 80°	<= 0.3	<= 50%	No	> 0.2	Yes		All
GOME-2A	01/01/2008 – 12/31/2016	< 80°	<= 0.3	<= 50%	No	> 0.2	Yes		All
OMI-QA4ECV ¹	01/01/2005 – 12/31/2017	< 80°	<= 0.3	<= 50%	No	> 0.2	Yes		6 - 21
OMI-NASA ¹	01/01/2005 – 12/31/2016	< 80°	<= 0.3	<= 50%			Yes	Yes	6 – 21
OMI-BEHR ¹	01/01/2005 – 12/31/2016	< 80°	<= 0.3	<= 50%			Yes	Yes	6 - 21

48 ¹ Rows 6-21 are selected to remove the anomalies developed in the OMI sensor (Boersma et al., 2018; Zhang et al., 2018).

49 **Table S4. Summary of annual trends of AQS NO₂ surface concentrations and satellite NO₂ TVCD products in each region during different periods¹**

		Northeast		Midwest		South		West	
		AQS site	CONUS	AQS site	CONUS	AQS site	CONUS	AQS site	CONUS
AQS NO ₂ VMR at 13:00 -14:00	2003 – 2011	-6.8 ± 0.7%		-6.1 ± 1.2%		-6.6 ± 0.7%		-7.6 ± 1.2%	
	2011 – 2017	-8.0 ± 1.2%		-6.4 ± 0.8%		-5.8 ± 0.6%		-7.2 ± 1.6%	
AQS NO ₂ VMR at 10:00 – 11:00	2003 – 2011	-6.6 ± 0.5%		-5.8 ± 1.5%		-6.5 ± 1.3%		-7.1 ± 1.6%	
	2011 – 2017	-7.6 ± 1.0%		-6.8 ± 0.5%		-5.7 ± 0.1%		-6.1 ± 1.1%	
SCIAMACHY	2003 – 2011	-17.1 ± 2.7%	-11.0 ± 3.3%	-12.9 ± 6.8%	-6.5 ± 0.8%	-9.1 ± 1.0%	-6.2 ± 1.5%	-9.1 ± 1.8%	-7.0 ± 1.4%
	2011 – 2017								
GOME2B	2003 – 2011								
	2013 – 2017	-11.4 ± 3.7%	-10.8 ± 3.9%	-9.9 ± 13.1%	-4.4 ± 27.2%	-8.9 ± 3.0%	-7.5 ± 3.6%	-11.8 ± 3.0%	-10.6 ± 2.3%
OMI-QA4ECV	2005 – 2011	-14.2 ± 6.3%	-10.6 ± 3.8%	-9.2 ± 4.2%	-8.4 ± 2.8%	-9.2 ± 2.7%	-8.2 ± 1.5%	-10.5 ± 1.6%	-8.7 ± 0.9%
	2011 – 2017	-18.0 ± 16.2%	-7.6 ± 4.2%	-7.6 ± 3.3%	-7.0 ± 1.7%	-4.8 ± 1.4%	-4.6 ± 1.0%	-6.4 ± 1.4%	-4.8 ± 1.2%
OMI-NASA	2005 – 2011	-11.8 ± 1.3%	-11.0 ± 1.8%	-10.9 ± 4.8%	-10.0 ± 4.1%	-10.0 ± 3.5%	-9.5 ± 1.9%	-10.2 ± 1.8%	-8.5 ± 0.9%
	2011 – 2016	-10.0 ± 4.9%	-8.5 ± 3.8%	-13.2 ± 3.2%	-9.2 ± 2.7%	0.3 ± 19.2%	-8.0 ± 5.5%	-9.0 ± 5.7%	-6.6 ± 3.9%
OMI-BEHR	2005 – 2011	-11.8 ± 1.8%	-10.9 ± 1.9%	-12.2 ± 7.3%	-9.8 ± 4.4%	-9.5 ± 3.1%	-8.8 ± 2.0%	-9.9 ± 1.1%	-8.2 ± 0.4%
	2011 – 2016	-8.2 ± 3.4%	-6.6 ± 1.7%	-27.4 ± 24.3%	-8.1 ± 3.0%	-7.2 ± 2.3%	-5.0 ± 1.3%	-13.2 ± 14.5%	-7.0 ± 4.8%

50 ¹ Annual trends are the averages of regional seasonal trends (e.g, Figure 7).

52 **References**

- 53 Acarreta, J. R., de Haan, J. F., and Stammes, P.: Cloud pressure retrieval using the O₂-O₂
54 absorption band at 477 nm, *J. Geophys. Res.-Atmos.*, 109, 10.1029/2003JD003915, 2004.
- 55 Boersma, K. F., Jacob, D. J., Eskes, H. J., Pinder, R. W., Wang, J., and Van Der A, R. J.:
56 Intercomparison of SCIAMACHY and OMI tropospheric NO₂ columns: Observing the diurnal
57 evolution of chemistry and emissions from space, *J. Geophys. Res.-Atmos.*, 113,
58 10.1029/2007JD008816, 2008.
- 59 Boersma, K. F., Jacob, D. J., Trainic, M., Rudich, Y., De Smedt, I., Dirksen, R., and Eskes, H. J.:
60 Validation of urban NO₂ concentrations and their diurnal and seasonal variations observed from
61 the SCIAMACHY and OMI sensors using in situ surface measurements in Israeli cities, *Atmos.*
62 *Chem. Phys.*, 9, 3867-3879, 10.5194/acp-9-3867-2009, 2009.
- 63 Boersma, K. F., Eskes, H. J., Dirksen, R. J., Veefkind, J. P., Stammes, P., Huijnen, V., Kleipool,
64 Q. L., Sneep, M., Claas, J., and Leitão, J.: An improved tropospheric NO₂ column retrieval
65 algorithm for the Ozone Monitoring Instrument, *Atmos. Meas. Tech.*, 4, 1905-1928,
66 10.5194/amt-4-1905-2011, 2011.
- 67 Boersma, K. F., Eskes, H. J., Richter, A., De Smedt, I., Lorente, A., Beirle, S., van Geffen, J. H.,
68 Zara, M., Peters, E., and Roozendael, M. V.: Improving algorithms and uncertainty estimates for
69 satellite NO₂ retrievals: results from the quality assurance for the essential climate variables
70 (QA4ECV) project, *Atmos. Meas. Tech.*, 11, 6651-6678, 10.5194/amt-11-6651-2018, 2018.
- 71 Bucsela, E. J., Krotkov, N. A., Celarier, E. A., Lamsal, L. N., Swartz, W. H., Bhartia, P. K.,
72 Boersma, K. F., Veefkind, J. P., Gleason, J. F., and Pickering, K. E.: A new stratospheric and
73 tropospheric NO₂ retrieval algorithm for nadir-viewing satellite instruments: applications to OMI,
74 *Atmos. Meas. Tech.*, 6, 2607-2626, 10.5194/amt-6-2607-2013, 2013.
- 75 Bucsela, E. J., Celarier, E. A., Gleason, J. L., Krotkov, N. A., Lamsal, L. N., Marchenko, S. V.,
76 and Swartz, W. H.: OMNO2 README Document Data Product Version 3.0, NASA, 38, 2016.
- 77 EUMETSAT: GOME_FACTSHEET, Germany, 33, 2015.
- 78 Kleipool, Q. L., Dobber, M. R., de Haan, J. F., and Levelt, P. F.: Earth surface reflectance
79 climatology from 3 years of OMI data, *J. Geophys. Res.-Atmos.*, 113, 10.1029/2008JD010290,
80 2008.
- 81 Krotkov, N. A., Lamsal, L. N., Celarier, E. A., Swartz, W. H., Marchenko, S. V., Bucsela, E. J.,
82 Chan, K. L., Wenig, M., and Zara, M.: The version 3 OMI NO₂ standard product, *Atmos. Meas.*
83 *Tech.*, 10, 3133-3149, 10.5194/amt-10-3133-2017, 2017.
- 84 Lamsal, L. N., Krotkov, N. A., Celarier, E. A., Swartz, W. H., Pickering, K. E., Bucsela, E. J.,
85 Gleason, J. F., Martin, R. V., Philip, S., and Irie, H.: Evaluation of OMI operational standard NO₂
86 column retrievals using in situ and surface-based NO₂ observations, *Atmos. Chem. Phys.*, 14,
87 11587-11609, 10.5194/acp-14-11587-2014, 2014.

- 88 Laughner, J. L., Zhu, Q., and Cohen, R. C.: The Berkeley High Resolution Tropospheric NO₂
89 product, *Earth System Science Data*, 10, 2069-2095, 10.5194/essd-10-2069-2018, 2018.
- 90 Lee, C., Martin, R. V., van Donkelaar, A., Richter, A., Burrows, J. P., and Kim, Y. J.: Remote
91 Sensing of Tropospheric Trace Gases (NO₂ and SO₂) from SCIAMACHY, in: *Atmospheric and*
92 *Biological Environmental Monitoring*, Springer, 63-72, 2009.
- 93 Marchenko, S., Krotkov, N. A., Lamsal, L. N., Celarier, E. A., Swartz, W. H., and Bucsela, E. J.:
94 Revising the slant column density retrieval of nitrogen dioxide observed by the Ozone
95 Monitoring Instrument, *J. Geophys. Res.-Atmos.*, 120, 5670-5692, 10.1002/2014JD022913,
96 2015.
- 97 Oetjen, H., Baidar, S., Krotkov, N. A., Lamsal, L. N., Lechner, M., and Volkamer, R.: Airborne
98 MAX-DOAS measurements over California: Testing the NASA OMI tropospheric NO₂ product,
99 *J. Geophys. Res.-Atmos.*, 118, 7400-7413, 10.1002/jgrd.50550, 2013.
- 100 Tilstra, L. G., Tuinder, O. N. E., Wang, P., and Stammes, P.: Surface reflectivity climatologies
101 from UV to NIR determined from Earth observations by GOME-2 and SCIAMACHY, *J.*
102 *Geophys. Res.-Atmos.*, 122, 4084-4111, 10.1002/2016JD025940, 2017.
- 103 Tong, D., Lamsal, L., Pan, L., Ding, C., Kim, H., Lee, P., Chai, T., Pickering, K. E., and Stajner,
104 I.: Long-term NO_x trends over large cities in the United States during the great recession:
105 Comparison of satellite retrievals, ground observations, and emission inventories, *Atmos.*
106 *Environ.*, 107, 70-84, 10.1016/j.atmosenv.2015.01.035, 2015.
- 107 Veefkind, J. P., de Haan, J. F., Sneep, M., and Levelt, P. F.: Improvements to the OMI O₂-O₂
108 operational cloud algorithm and comparisons with ground-based radar-lidar observations, *Atmos.*
109 *Meas. Tech.*, 9, 6035-6049, 10.5194/amt-9-6035-2016, 2016.
- 110 Wang, P., Stammes, P., van der A, R., Pinardi, G., and van Roozendael, M.: FRESCO+: an
111 improved O₂ A-band cloud retrieval algorithm for tropospheric trace gas retrievals, *Atmos.*
112 *Chem. Phys.*, 8, 6565-6576, 10.5194/acp-8-6565-2008, 2008.
- 113 Wang, Y., Beirle, S., Lampel, J., Koukouli, M., De Smedt, I., Theys, N., Ang, L., Wu, D., Xie, P.,
114 and Liu, C.: Validation of OMI, GOME-2A and GOME-2B tropospheric NO₂, SO₂ and HCHO
115 products using MAX-DOAS observations from 2011 to 2014 in Wuxi, China: investigation of the
116 effects of priori profiles and aerosols on the satellite products, *Atmos. Chem. Phys.*, 17, 5007,
117 10.5194/acp-17-5007-2017, 2017.
- 118 Williams, J. E., Scheele, M. P., van Velthoven, P. F. J., Cammas, J.-P., Thouret, V., Galy-Lacaux,
119 C., and Volz-Thomas, A.: The influence of biogenic emissions from Africa on tropical
120 tropospheric ozone during 2006: a global modeling study, *Atmos. Chem. Phys.*, 9, 5729-5749,
121 10.5194/acp-9-5729-2009, 2009.
- 122 Williams, J. E., Boersma, K. F., Sager, P. L., and Verstraeten, W. W.: The high-resolution version
123 of TM5-MP for optimized satellite retrievals: description and validation, *Geoscientific Model*
124 *Development*, 10, 721-750, 10.5194/gmd-10-721-2017, 2017.
- 125 Zara, M., Boersma, K. F., De Smedt, I., Richter, A., Peters, E., Van Geffen, J. H. G. M., Beirle,
126 S., Wagner, T., Van Roozendael, M., and Marchenko, S.: Improved slant column density retrieval

127 of nitrogen dioxide and formaldehyde for OMI and GOME-2A from QA4ECV: intercomparison,
128 uncertainty characterization, and trends, Meas. Tech. Discuss, 1-47, 10.5194/amt-11-4033-2018,
129 2018.

130 Zhang, R., Wang, Y., Smeltzer, C., Qu, H., Koshak, W., and Boersma, K. F.: Comparing OMI-
131 based and EPA AQS in situ NO₂ trends: towards understanding surface NO_x emission changes,
132 Atmos. Meas. Tech., 11, 3955-3967, 10.5194/amt-11-3955-2018, 2018.

133